Paleolakes of Northeast Hellas: Precipitation, Groundwater-Fed, and Fluvial Lakes in the Navua–Hadriacus–Ausonia Region, Mars

Article *in* Astrobiology · October 2018

DOI: 10.1089/ast.2018.1816

CITATIONS
9

READS
261

3 authors:

Henrik Hargitai
Eötvös Loránd University
473 PUBLICATIONS **459** CITATIONS
SEE PROFILE

Virginia Gulick
SETI Institute
210 PUBLICATIONS **5,226** CITATIONS
SEE PROFILE

Natalie Glines
SETI Institute
28 PUBLICATIONS **199** CITATIONS
SEE PROFILE

ASTROBIOLOGY
Volume 18, Number 11, 2018

DOI: 10.1089/ast.2018.1816

Research Article

Paleolakes of Northeast Hellas: Precipitation, Groundwater-Fed, and Fluvial Lakes in the Navua–Hadriacus–Ausonia Region, Mars

Henrik I. Hargitai,[1,2] Virginia C. Gulick,[1,3] and Natalie H. Glines[1,3]

Abstract

The slopes of northeastern Hellas Basin, Mars are rich in exhibit a wide variety of fluvial landforms. In addition to the Dao–Niger–Harmakhis–Reull Valles outflow channels, many smaller channels and valleys cut into this terrain, several of which include discontinuous sections. We have mapped these channels and channel-associated depressions to investigate potential paleolakes from the Navua Valles in the West, through the Hadriacus Mons volcano in the center, to the Ausonia Montes in the East. We have identified three groups of candidate paleolakes at the source regions of major drainages and a fourth paleolake type scattered along the lower reaches of these drainages. Each paleolake group has a distinct character, determined by different formative processes, including precipitation and groundwater for lakes at the channel sources, and fluvially transported water at the lower channel reaches. Only one of these 34 basins had been cataloged previously in paleolake basin databases. Several of these sites are at proximity to the Hadriacus volcanic center, where active dikes during the Hesperian could have produced hydrothermal systems and habitable environments. Deposits within these paleolake depressions and at the termini of channels connected to these candidate paleolakes contain the geological and potentially biological record of these environments. Key Words: Mars—Geology—Geomorphology—Fluvial processes—Paleolake—Astrobiology. Astrobiology 18, xxx–xxx.

1. Introduction

MARS HAS HOSTED a large number of lakes throughout its history (Cabrol and Grin, 1999, 2001, 2010; Goudge *et al.*, 2015), from Noachian-aged oceans (Parker *et al.*, 1989; Gulick and Baker, 1990; Baker *et al.*, 1991) to sea-sized lakes (Irwin *et al.*, 2002), to Noachian–Hesperian lakes (*e.g.*, Grant *et al.*, 2011), to small lake chains formed in the Hesperian–Amazonian transition (Wilson *et al.*, 2016). Paleolakes are fed by valley networks (Fassett and Head, 2008) and groundwater sources (*e.g.*, Wray *et al.*, 2011).

The thickest lacustrine sediments observed on Mars occur on the North Hellas highlands in Terby crater (Ansan *et al.*, 2011), which is filled with mid-to-late Noachian-layered material (Wilson *et al.*, 2007). Hellas Basin, the deepest depression on Mars, was also probably a lake in the Noachian (Malin and Edgett, 2000; Moore and Wilhelms, 2001; Wilson *et al.*, 2010).

The terrain of the Navua Valles–Hadriacus Mons–Ausonia Montes (NHA) region slopes toward Hellas Basin from the northeast. In our previous study (Hargitai *et al.*, 2017), we mapped this area and identified discontinuous outflow channels, both medium-sized and narrow single channels, integrated valley networks, unchanneled valleys, and sinuous pit chains. These landforms provide evidence for both significant surface runoff and subsurface flow, probably from precipitation and hydrothermal groundwater outflow. In this study, we investigated whether there were any depressions connected to these channels, where water potentially ponded and created environments that were habitable for longer periods than the channel floors.

In a 660,000 km^2 area previously not considered particularly rich in paleolake basins, we identify 34 candidate paleolakes that are between 3 and 77 km in diameter. More than half of the depressions with inlet and/or outlet channels also have delta-like deposits at the terminus of the inlet channel, and so are the most likely candidates for paleolakes. We have determined the crater retention ages of the paleolake floors and calculated the minimum volumes of the basins assuming water infill at the elevation of inlet or outlet channels. Our detailed geomorphological study to identify the likely origin of the lakes has revealed a complex, multisource, episodic lacustrine history of

[1]NASA Ames Research Center, Space Science Division, Moffett Field, California.
[2]Department of Media and Communication, Eötvös Loránd University, Budapest, Hungary.
[3]SETI Institute, Mountain View, California.

this region, which lasted from the Hesperian to possibly the Late Amazonian period (Hartman and Neukum, 2011).

In our study region, three paleolakes were previously noted: N10 (Cabrol and Grin, 2001), and Ausonia and Peraea Cavi (Hamilton *et al.*, 2015). The large number of candidate paleolakes identified in this study using Mars Reconnaissance Orbiter (MRO) Context Camera (CTX) images suggests that the regional, or even global, number of paleolake and paleodrainage systems is significantly higher than that previously thought.

2. Methods

2.1. Paleolake identification

We delineated lake outlines based on the presence of specific morphological features, which include termini or emergence of inlet or outlet channels, benches, and delta-shaped terminal deposits with steep frontal scarps within the basins. We used drainage data from our previous geological mapping (Hargitai *et al.*, 2017) conducted at ~1:60k digital scale to map channel networks at CTX resolution. We have tested all channels' start and end points on Mars Global Surveyor (MGS) Mars Orbiter Laser Altimeter (MOLA) data to determine if there is an adjacent basin at the origin or terminus of the channel. We surveyed km-scale depressions some of which could be identified in MOLA data, without having visibly distinct perimeters in CTX or HiRISE images. We call these features ''topographic basins'' to distinguish them from paleolakes in impact craters and steep-walled cavi.

Following topographic basin identification, minor inlet or outlet channels were often able to be identified. We could not identify closed lakes fed only by groundwater without an outlet channel with this method but could detect groundwater-fed lakes with any outlet channel. We identified a contour line that touches the inlet channel termini or bench on a MOLA gridded Digital Terrain Model (DTM). Where the basin had an outlet or inlet channel and a bench at two different elevations, we created both a ''high stand'' outline that represented overspill water levels and a ''low stand'' outline that represented water level that putatively formed the bench. We assumed that all basins with an inlet channel could have contained a lake (see *e.g.*, Goudge *et al.*, 2015).

2.1.1. Size and volume considerations. Our lake volume calculations are conservative, because we assumed that channels are subaerial without subaquatic reaches. In these calculations, we included the entire terminal deposit(s) where possible, the elevation of which would indicate the largest extent of a paleolake. This ''best-fit'' contour was the maximum area contour that did not spill into surrounding plains in the MOLA gridded DTM. This introduced several inconsistencies with the morphological data due to low MOLA DTM resolution (100 m/px) and interpolation, but it still provided a reasonable approximation of the scales of lake volumes and areas, which were, naturally, variable (Fig. 1).

The resulting paleolake outlines in many places contained several different geomorphic units, such as outcrops of

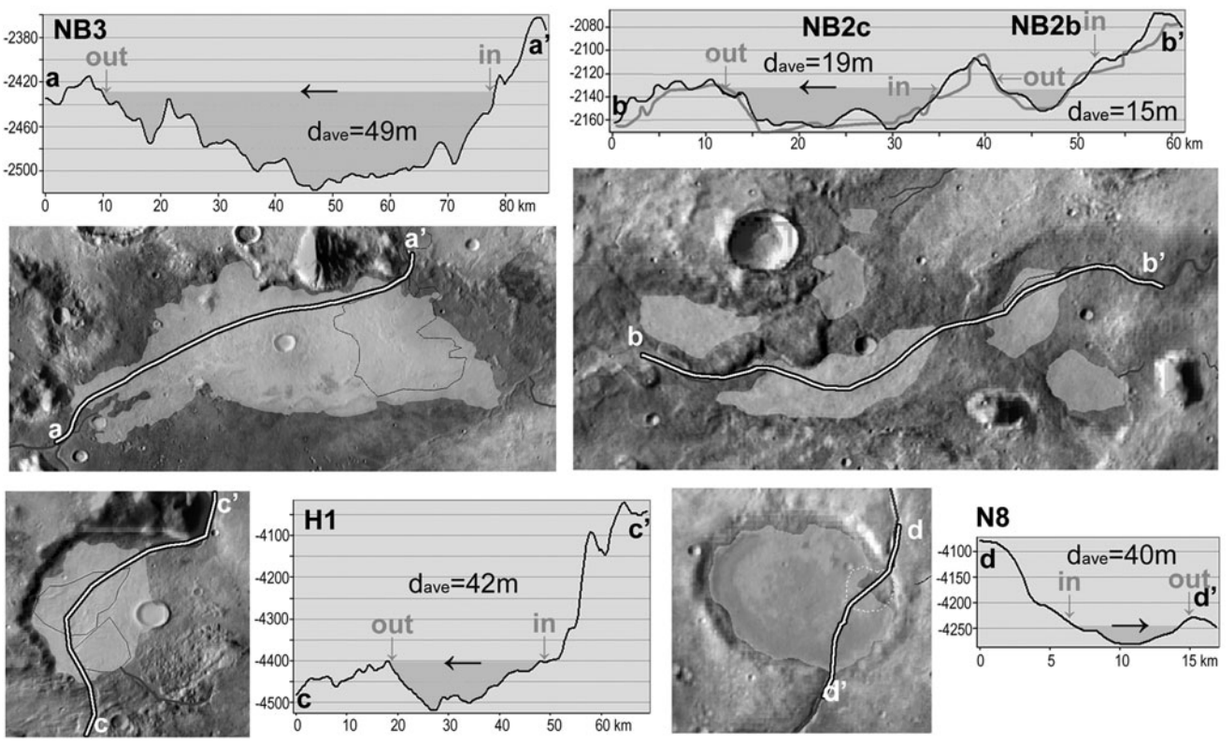

FIG. 1. Selection of lake profiles. Labels refer to lake IDs used in this study. ''In'' and ''Out'' show the junctions of the inlet and outlet channels, respectively. Yellow Bright lines with black outlines show the profile tracks. Letters **a–d** and **a'–d'** indicate the left and right end points, respectively, of the profiles in the cross sections and the corresponding images. Light toned (blue) areas represent the measured extent of candidate paleolakes. d_{ave} is the average depth. For the NB2 lakes, green (lower) line shows MOLA PEDR data profile. Arrows show the direction of flow. Background: Mars Orbiter Laser Altimeter (MOLA) Digital Terrain Model (DTM) where purple is low, brown is high.

bedrock and sediments. This suggests that these basins have been modified during postlacustrine landscape evolution. These strata may have been already present during the active lake phase, or may have been deposited or exhumed afterward. Paleolake depth reconstructions depend on geological factors that either decrease or increase the resulting values. The volume calculation method itself produces a ''minimum eroded volume.'' Bank wall erosion could significantly *decrease* slopes or even depths measurable at present due to infilling. Atmospherically emplaced deposition of mantle material could likewise decrease measurable depths. In contrast, postlacustrine impact cratering would form lake bed depressions that *increase* the paleolake depth measurement and predicted water volume.

3. Classification of Lake Depressions

The criteria we used for identifying potential paleolake basins are that it should be (a) a depression, and (b) associated with at least one channel (inlet or outlet).

The presence of an inlet channel suggests that the basin received water from that channel, while an outlet channel indicates that water overtopped and eroded through the basin rim.

Paleolakes can be classified into hydrologically open-basin (balanced fill) lakes or closed-basin (endorheic) lakes (*e.g.*, Nichols, 2009:152). Open lakes on Earth connected by inlet and outlet channels generally transport fresh water, whereas closed lakes become progressively more saline with increasing evaporation. Closed lakes on Mars might have remained stable on the surface for a slightly longer period than inlet–outlet lakes with lower salinity, if present though the more recent Amazonian climate.

Hydraulic conditions of lakes are difficult to infer even on Earth (Costelloe *et al.*, 2009). In this study, we use the terms ''open'' and ''closed'' basin to refer to the presence or absence of inlet and outlet channels associated with the depression. Apparently closed mesoscale basins on a sloping terrain may have been fed or drained by subsurface inflow or outflow and would therefore have been hydraulically open (Sanford and Wood, 1991), as indicated in regions where we found concentrations of lakes connected by only short, minor channels. These are therefore not necessarily endorheic, even though they are topographically terminal lakes for surface flows. Hydraulically closed basins may have formed in Hellas Basin, which is the ultimate base level in this region.

We have classified basins into the following types (Table 1 and Fig. 2): open-basin lakes (source and through-flowing) and closed-basin lakes (terminal and independent).

3.1. Open-basin lakes

Open-basin lakes (Cabrol and Grin, 1999; Goudge *et al.*, 2012) are situated in basins possessing an outlet. While channels that emerge on flat terrain may be fed by various surface or subsurface sources, channels that emerge at the rim of a basin are sourced from that basin lake, unless the basin was completely filled with erodible material at the time when the channel formed. The presence of an outlet channel suggests that the water level exceeded the lowest elevation of the basin rim, over spilled and eventually eroded a valley head at the outlet (Fassett and Head, 2008; Goudge *et al.*, 2012). The discharge of the outlet channel is related to the highest gain of water from all sources in the lake.

Alternatively, a channel can also erode back into and breach the crater rim by several processes, including groundwater sapping, piping, or ice-rich mass wasting processes. Outlet channels in the mapped region are not deeply cut into the basin rims suggesting formation by overspill.

We have categorized open-basin lakes into two categories:

1. Source lakes with only outlet but no inlet channels (''valley-head basins,'' De Hon, 1992). A source lake can be fed by a variety of water processes, including groundwater, surface water, or melt-water flows from a snow or ice body accumulated in the basin. On Earth, this morphology characterizes dominantly groundwater-fed ''spring lakes'' with substantial outlets and ''drained lakes'' with minor outlets (WDNR, 2001).
2. Through-flowing lakes with both inlet and outlet channels (Forsythe and Blackwelder, 1998, ''intra-valley basin,'' De Hon, 1992), at the same elevation, receive most of their water from surface flows. This type is also called a ''drainage lake'' on Earth (WDNR, 2001), where the groundwater table does not intersect the lake but is, instead, located at some distance below the elevation of the lake bottom. These lakes can recharge the groundwater system. A majority of these putative lakes are part of valley-lake-chain systems on Mars (Fassett and Head, 2008). A potential paleolake-chain system also occurs in our study region.

3.2. Closed-basin lakes

On Earth, closed-basin lakes in arid climate at the terminus of surface or subsurface flow systems form playas. Ephemeral or playa lakes in arid zones dry out periodically during their lifetime, where rainfall is irregular and evaporation is high, producing evaporites (*e.g.*, Nichols, 2009:152) that can be spectrally detected. Closed-basin lakes (Aureli *et al.*, 2014) also have two types:

3. Terminal lakes (''valley-terminal basins,'' De Hon, 1992) have inlet valleys, and no outlets, and are typically situated in impact craters on Mars. In arid climates on Earth, this setting is typical of dry playas that are supported by surface inflow. Lake water infiltrates into a deeper, disconnected, groundwater table (Forester *et al.*, 2003; Tyler *et al.*, 2006).
4. Independent lakes (''isolated basins,'' De Hon, 1992) have no inlet or outlet valleys, are sourced from groundwater or precipitation in the form of rain or accumulated snow/ice in the basin, and are not connected directly to surface drainage. On Earth, this landlocked morphology is typical of ''seepage lakes'' where water level is maintained by the groundwater table (WDNR, 2001). In arid climates, groundwater-fed lakes form wet playas characterized by evaporites (Forester *et al.*, 2003; Tyler *et al.*, 2006), brines, and soil salinization (Costelloe *et al.*, 2009). Lakes with only minor, short inlet channels can indicate that it was dominantly sourced from groundwater (Fassett and Head, 2008) (see also Section 5.7).

Table 1. Properties and Types of the Putative Paleolake Basins

Group	ID	Longitude (E°)	Latitude (°)	Maximum D (km)	Elevation (m) (MOLA)	Maximum depth (m)	Average depth (m)	Area (km^2)	Volume (km^3)	Host	Type	Complexity index
Ausonia	A1	95.8	−28.9	29	−1053	134	31	231	8	T	**O/T**	2
	A2H	95.4	−29.7	51	−1394	1021	696	1319	1055	CA	**O/T**	2
	A2L				−2008	331	224	928	239			
	A3	95.2	−30.4	32	−1821	271	102	277	33	T	**O/T**	2
	A4	95.6	−31	32	−2120	698	176	363	74	T	?	5
	A5	95.6	−32	6	−2165	173	81	27	2	Ot	**O/T**	2
	A6	96.5	−32	56	−2320	404	266	960	256	CA	?	0
Hadr.	H1	87.3	−35.9	23	−4404	169	42	338	16	C/S	**O/T**	3
	(H2)	85.9	−36.2	17	−4913	51	13	102	2	T	**O/T***	2
	H3	85.2	−36.5	7	−5081	207	74	30	3	C	C/T	2
Navua A	N1	83.2	−27.4	77	−2130	891	143	3144	495	C	C/T	3
	N2	83.4	−28.4	20	−1770	452	123	262	33	C	C/T	2
	N3 L	84.3	−29.1	54	−2818	171	71	478	39	C/S	C/T	1
	N3H				−2630	629	157	1307	234			
	N4	83.7	−29.8	27	−2862	246	73	235	19	C/S	C/T	1
	N5	83	−29.8	26	−2772	176	83	249	24	C/S	C/T	1
	N6	82.1	−30.5	21	−2465	98	31	258	9	C	**O/T**	2
	N7	81.9	−31.6	8	−3850	63	16	40	1	T	C/T	2
	N8	81.3	−32.1	14	−4240	91	40	122	6	C	**O/T**	5
	N9	81	−33.4	7	−5239	37	12	9	0.1	C/S	**O/T**	3
	N10H	80.9	−33.8	34	−5446	119	51	118	2	C/S	**O/T**	3
	N10 L				−5480	84	39	144	7			
	(N11)	79.4	−35.3	22	−6345	108	31	248	9	T	**O/T***	2
	N-A1	80.7	−30.4	8	−3064	55	26	37	1	T	O/S	1
	N-A2	80.3	−30.5	12	−3073	61	27	54	2	T	C/T	0
Navua B	NB1	87.1	−30.3	21	−2011	26	12	105	1	T	O/S	2
	NB2a	88.6	−31.1	8	−2109	13	7	34	0.3	T	C/T/I	0
	NB2b	88.4	−31	10	−2125	37	15	46	1	T	**O/T**	2
	NB2c	88.1	−31.1	21	−2134	38	19	105	2	T	**O/T**	2
	NB2d	88.1	−30.8	3	−2115	7	3	6	0.02	T	C/T	0
	NB2e	88.1	−30.9	7	−2120	29	14	28	0.4	T	C/I	0
	NB2f	87.8	−31	10	−2150	55	20	45	1	T	O/S	1
	NB3	86	−31.4	74	−2426	351	49	1461	84	T	**O/T**	2
	(NB4)	84	−32.6	15	−2804	37	11	51	1	T	**O/T***	1
	NB5	84.4	−33.3	16	−4040	148	51	96	6	C/S	C/T	0
	NB6	81.4	−35	8	−5858	74	30	38	1	Ot	C/T	2
	NB7	81.8	−35.2	14	−5860	28	13	77	1	Ot	C	1

ID: First letter refers to group (A, Ausonia; H, Hadriaca; N, Navua A; and NB, Navua B); last letter L shows outlines at low stand water level, H is at high stand water level. D, diameter. Host: C, crater; C/S, crater sub-basin; Ot, Other; T, topographic basin (nonimpact); CA, Cavi. Type: O, open; C, closed. O/T, through-flowing; O/S, source lake; C/I, independent; C/T, Terminal. Asterisks (*) indicate potential alluvial basins. Maximum depth values include those measured in postlacustrine craters. Complexity index is the number of morphological feature types indicative of lacustrine processes, additional to depression and connected channel morphologies. Higher numbers indicate higher confidence in lacustrine origin.

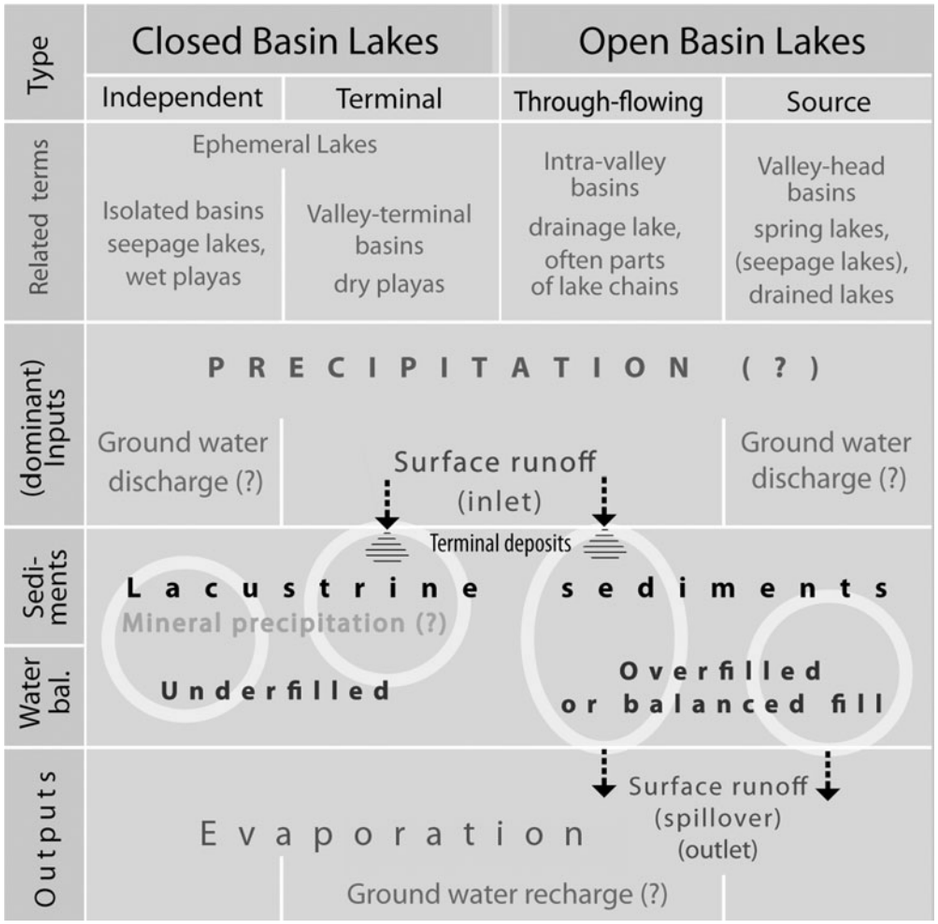

FIG. 2. Lake types and characteristics, based on Bohacs *et al.* (2000) (water balance), and Sanford and Wood (1991), modified. See the text for discussion.

In the mapped area, we identified an intermediate situation where closed-basin lakes may be fed by water infiltrated from nearby lakes that are in turn fed by occasionally active surface drainage.

4. Candidate Paleolakes of the NHA Region

We have identified 19 potential open-basin lakes and 14 closed-basin lakes in the NHA region (Figs. 3 and 4, and Table 1, Table 2). While many candidate paleolake basins are ''topographic depressions'' in rolling terrain, 12 are located in impact craters, and 2 are in steep-sided oval depressions (cavi). Half of the candidate paleolakes are through flowing with inlets and outlets, one third is terminal, 10% are source lakes, and 6% are independent.

4.1. Complexity index

We have calculated relative paleolake confidence levels by adding the number of present morphological paleolake indicators, including long inlet channels, outlet channels, putative deltas, layered deposits, and benches. Since these morphologies can be produced by a variety of processes, this confidence index rather expresses the complexity of the system, and not necessarily a lacustrine origin. While both an inlet and an outlet provide high confidence of the existence of a paleolake, inlet channels alone may form without producing a standing body of water in a closed basin. Therefore, they are only candidate paleolakes (Goudge *et al.*, 2015) even if they contain a terminal deposit that may be either a delta or a subaerial fan.

5. Morphological and Other Features

We identified paleolakes based on their morphological features (Kereszturi and de Hon, 2014). In this study, we interpreted all channel-associated depressions as candidate paleolakes.

We have cataloged the following features (Table 3): (1) valleys or channels adjacent to or within depressions, interpreted as an inlet or outlet (De Hon, 1992; Fassett and Head, 2008) consistently at similar elevations (Scott *et al.*, 1992); (2) flat-surfaced fan-shaped deposits interpreted as potential deltas or fans and radiating terminal deposits with lineations interpreted as flowlines (Cabrol and Grin, 2000; Ori *et al.*, 2000; Schon *et al.*, 2012); (3) benches or terrace-like features (Ori *et al.*, 2000; Irwin *et al.*, 2005); (4) smooth plains in depressions interpreted as potentially lacustrine/

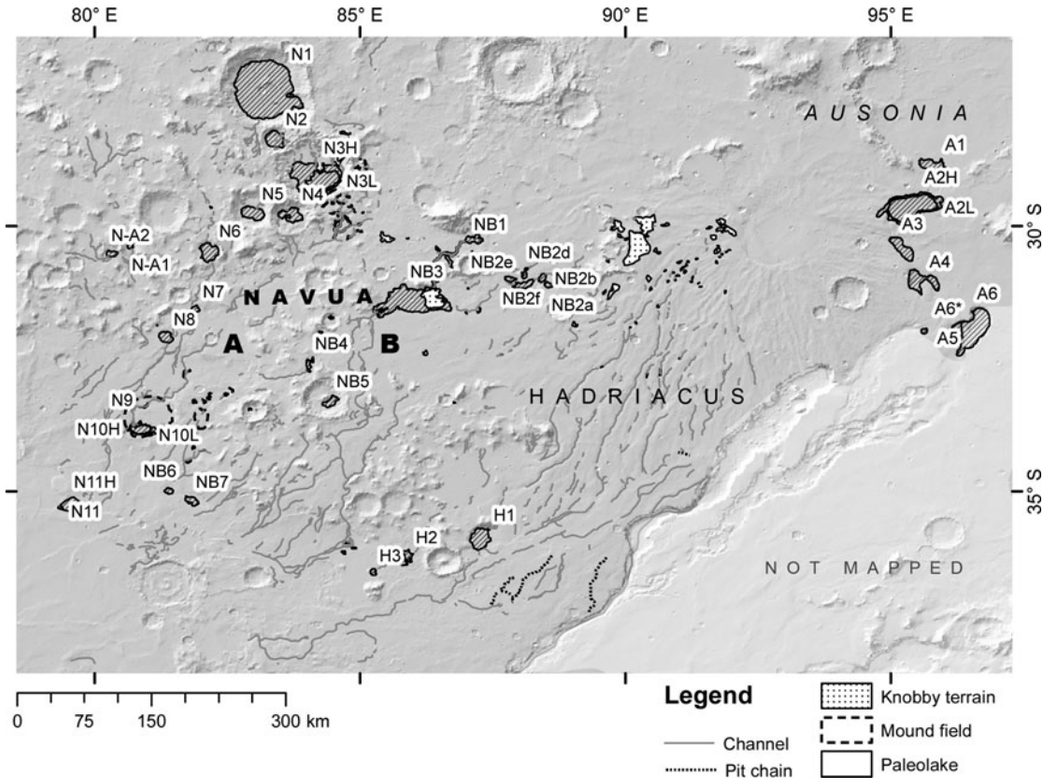

FIG. 3. Geographic map of the NHA region showing the identified candidate paleolake basins, fluvial systems (Hargitai *et al.*, 2017), and potentially related terrain features. Navua: Navua Valles, Hadriacus: Hadriacus Mons, Ausonia: Ausonia Montes. Background: THEMIS day IR mosaic.

playa sediments (De Hon, 1992; Scott *et al.*, 1995); and (5) layered deposits (Goudge *et al.*, 2012), including light-toned deposits (LTDs). Two additional features are potentially related to lacustrine processes: (6) concentric patterned ground interpreted as periglacial shoreline features and (7) basin extensions interpreted as collapse troughs.

5.1. Channels or valleys

In their global closed-basin lake survey, Aureli *et al.* (2014) distinguished short inlet channels (<10 km) that typically terminate in pristine impact craters, and long inlet channels that are similar to valley networks and usually terminate in degraded craters. Both types occur in our mapping area.

Open or closed basins with inlet valleys may be fed by surface flow, groundwater, melt water, or direct precipitation. The position of the depression–channel associations interpreted as open or closed may have resulted from an overprinting of geomorphic features over time that may have been active separately at different stages of lacustrine evolution. For example, inlet channels may have been active at different times than outlet channels of the same depression; however, this is less likely than a coevolving scenario. Lakes may have transitioned from one type to another with changing hydrological conditions over time. Postlacustrine processes may have subsequently modified topography.

From 11 basins with both inlet and outlet channels (32% of all basins), we determined that the inlets are slightly larger ($\sim$1.1 times) than their outlets (Fig. 5). This suggests that inflow and outflow were approximately similar, which is consistent with a lacustrine model and coexistence of the inlet and outlet channels. It also suggests that the effects of infiltration, groundwater outflow, and evaporation may have been negligible, or that there was a persistent inflow, which balanced out the potential losses, or that these basins were overfilled. The short length of several basin's inlet channels suggests that perhaps in these lakes, water volumes probably originated mostly from groundwater, and only a smaller fraction was supplied by surface channels.

Our analysis is based on gridded MOLA data that in places are less consistent with MOLA track areolocated Precision Experiment Data Record (PEDR) laser altimetery measurement data points. PEDR point distribution is too sparse for producing contour lines of the paleolakes. Accurate MOLA PEDR elevation data, where available at inlet/outlet junctions, show that outlet junctions are at 14 m lower than inlets on average (extremes: 8 m higher and 64 m lower) (Table 2). The elevations of the outlet channel floors are probably lower than those of the inlets, because outlets were incised, while inlets in many placed deposited sediments at its lake junction. In three open basins (NB4, N11, and H2), the PEDR elevation difference between outlet and inlet junction elevation is twice as much as the average lake depth calculated from MOLA

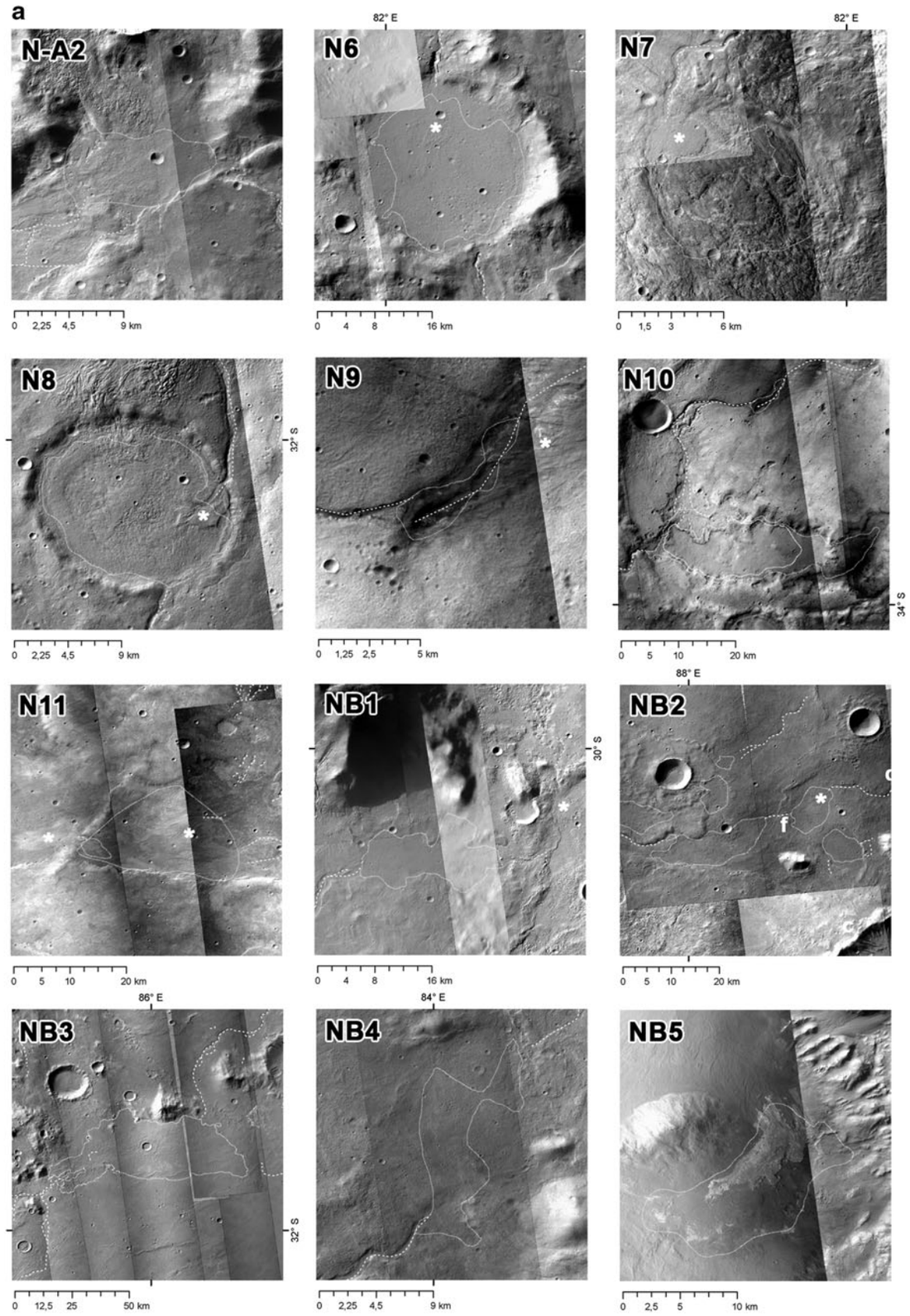

Figure 4a. (continued)

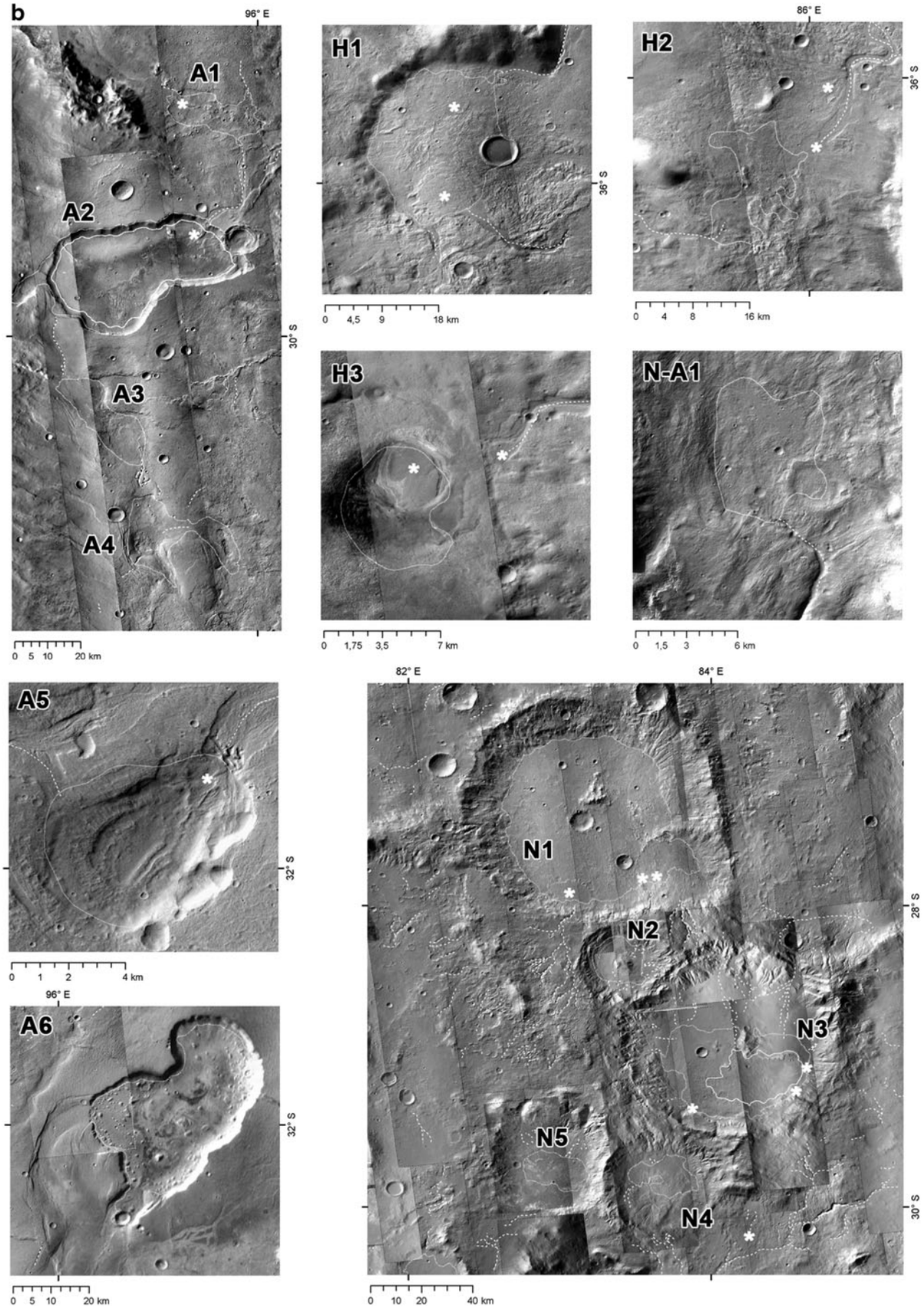

Figure 4b. (continued)

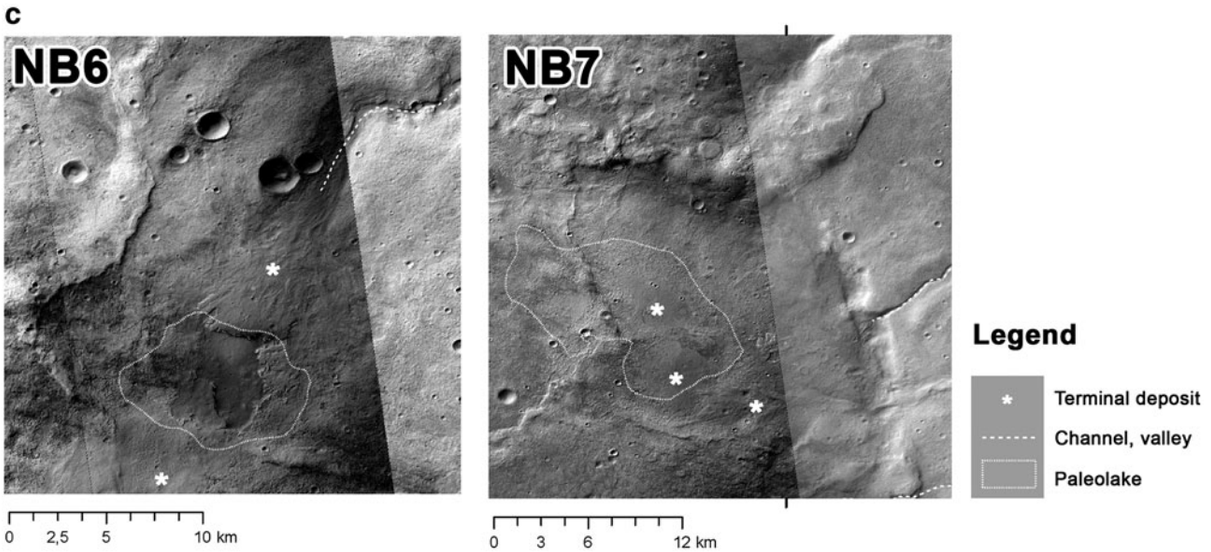

FIG. 4. Sketch Maps of the individual paleolake depressions over CTX mosaic. Dotted outlines: putative paleolake boundaries based on MOLA data; dashed outlines: channels; askeriks: terminal deposits.

data. In these cases, even considering incision, it is more likely that these basins were not lacustrine, and channels downslope have formed from groundwater seepage or snowmelt, or they (*e.g.*, H2) comprised of adjacent sub-basins at different levels connected by subsurface flow. Where the average calculated depth is 50% higher than the difference between inlet and outlet junction elevations, lacustrine origin is more likely. Some outlet channels (*e.g.*, in the NB2 lake group) may have only functioned as occasional flood spill channels, but water was primarily transported in the subsurface to the adjacent lake at lower elevation. Alluvial deposition and flooding followed by groundwater seepage may alternate, as seen on Earth (see section 5.7).

The average inlet channel width was 551 m, whereas the average outlet width was 657 m (sample size: 32 inlet and 20 outlet). Approximately half of all depressions had outlet channels and 85% had inlet channels. Twenty-one percent of the depressions had two or three inlet channels, which may or may not have been active simultaneously (Table 4).

As with trends for impact craters, we observe a paucity of small channels on ancient (Noachian–Hesperian) terrain on Mars. The narrowest inlet channel in our mapped region is 100 m wide, identified on 6 m/px CTX imagery. This suggests that channels smaller than this size were removed by, for example, erosion (*e.g.*, Craddock and Maxwell, 1993), terrain softening (Jankowski and Squyres, 1993), or with the

Table 2. Elevations of Inlet and Outlet Channels of Open Basins, from Mars Orbiter Laser Altimeter Track PEDR Data

	Average depth	*Inlet 1 elevation (m)*	*Inlet 2 elevation (m)*	*Outlet elevation (m)*	*Elevation difference (m)*	*Elevation difference% of average depth (%)*
A1	31	–1065	–1062	–1057	8	26
A2H	696	–1286		–1322	–36	–5
A3	102	–1826		–1813	13	13
A5	81	–2125		n/a		
H1	42	–4405	–4419	–4405	0	0
H2	13	–4910		–4933	–23	–177
N6	31	–2456		n/a		
N8	40	–4248		–4241	7	18
N9	12	–5241		–5245	–4	–33
N10H	51	–5436		–5436	0	0
N11	31	–6348		–6412	–64	–206
NB2b	15	–2133		–2134	–1	–7
NB2c	19	–2142		–2146	–4	–21
NB3	49	–2417	–2392	–2442	–25	–51
NB4	11	–2790		–2811	–21	–191

Where the elevation difference is higher than the average depth calculated from Mars Orbiter Laser Altimeter Mission Experiment Gridded Data Record (MEGDR) data, we consider those basins alluvial.

Table 3. Morphologic AL Features of the Candidate Paleolake Basins

ID	*Lake Night IR 1-high 2-med 3-low*	*Inlet channel width, m*	*Outlet channel width, m*	*Number of inlets, L-long*	*Long inlet?*	*Number of outlets*	*Number of deltas*	*Bench/ terrace*	*Smooth interior deposit*	*Layer*	*LTD cliff*	*Nondeltaic terminal deposit*	*Any terminal deposit*	*Ring of rough terrain*	*Basin Appendix*	*Confidence, 0-low, 5-high*
A1	2	250	240	2		1		+			+	+	+			2
A2L	1	2400	320	1L	+	1						+	+		+	2
A3	3	420	420	1		1	1				+		+			2
A4	2	220/250/450	2200 (?) Inverted	3		?	3	+		+	+	+	+			5
A5	3	1900	970	1		1		+				+	+			2
A6	1		4500			?									+	0
H1	2	870/1400	1300	2L	+	1	1					+	+			3
H2	2	1900	1050	Close L	+	1						+	+			2
H3	3	900		Close L	+		Multiple			+	+		+			2
N1	2	520/770/others		2L	+		2						1			3
N10L	2	570	610	1L	+	1			+		+	+	+			3
N11	3	460/120	320	1L	+	1						+	+			2
N2	2	gullies, fan channels			many small			+	+							2
N3L	2	gullies, fan channels			many small		1					+	+			1
N4	1	240		2				+			+					1
N5	1	160		2				+			+					1
N6	2	260	250	1L	+	1						+	+			2
N7	2	340		1L	+		1						+			2
N8	2	370/140	390	1		1	1	+	+	+			+	+		5
N9	2	?	500	1L	+	1		+			+	+	+			3
N-A1	3		270			1										1
N-A2	3	160/280		1		?					+					0
NB1	3	100	200	?		1			+							2
NB2a	3	190/200/280		3												0
NB2b	3	170	190	1L	+	1						+	+	+		2
NB2c	3	320	540	1L	+	1										2
NB2d	3			1										+		0
NB2e	3															0
NB2f	3		260			1										1
NB3	3	770	500	1L	+	1						+	+			2
NB4	2	260	310	1		1										1
NB5	1							Close			+	+	+			0
NB6	3			Close L	+				+		+	+	+			2
NB7	1–3			Close					+			+	+	+		1
Total				29	14	18	7	8	5	3	11	15	20	3	2	
%				85 L 41	41	53	21	23	15	8.	32	44	59	8.	5.9	
Average		551	657													

[+]Symbol refers to the presence of a feature. "Close L" refers to a nearby, long inlet.

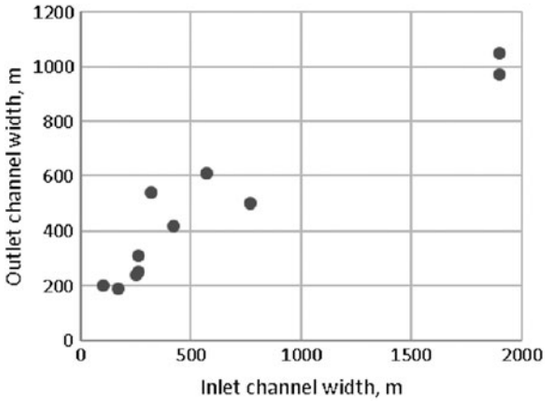

FIG. 5. Relation of inlet and outlet channel widths for the 11 basins that exhibit both inlet and outlet channels.

removal of a thick ice layer in which these features formed (Weiss and Head, 2015). The removal is likely related to channel depth corresponding to 100 m width. In the Navua Valles region, the smallest channel is 15 m wide, which suggests that those are younger than lake-inlet channels. Alternatively, lake-associated fluvial pathways only formed from larger discharges, for example, floods.

5.2. Terraces

Terraces or benches are morphological evidence of a period of prolonged, stable water level, where infiltration and evaporation rates kept pace with inflow and outflow volumes. Bench-like features may include those in weathering sequences that are globally distributed in irregular basins. However, these depressions likely formed by erosion and not by lacustrine deposition (Carter *et al.*, 2015). Benches also form where a resistant stratigraphic layer is present at the center of the basin. This stratum can provide a temporary barrier to subsequent basin infilling by alluvial or mass wasting processes. Such a layer could also have been ice rich, which, upon melting, formed a temporary lake (*e.g.*, lakes A4, A5, and N9; see Fig. 4 for additional examples).

Leverington and Maxwell (2004) interpreted craters that are characterized by crater fill terraces, and inlet and outlet valleys as volcanic, involving the flow and ponding of lava. In their model, inner terraces formed by subsidence and drainage of volcanic material. We could not identify potentially volcanic channel sources (*e.g.*, pits) and channel-associated volcanic deposits in this terrain, although we identified such features elsewhere on Mars (Hargitai and Gulick, 2018).

We identified benches or terraces in 23% of the depressions. Some have subdued edges, while others are sharp, which may imply different compositions or that there were prolonged periods between their formation. Regardless of the exact processes responsible for their formation, these terraces underwent both collapse and erosion.

Table 4. Presence and Type of Inlet or Outlet Channels in the Candidate Paleolake Basins, and Their Percentage

	%
0 Inlet channel	15
1 Inlet channel	44
2 Inlet channels	15
3 Inlet channels	6
Inlet channel terminates at a distance	12
Short inlet channels	6
Long inlet channel	41
Outlet channel	53
Inlet channel with terminal deposit	68

5.3. Deposits

5.3.1. Terminal deposits. We identified flat-surfaced, delta-like terminal deposits in 20% of the depressions and terminal deposits with flowlines radiating from the channel termini in 44% of the basins. Combined, 60% of the basins exhibit terminal deposits, while such deposits are absent in 32% of inlet channels.

Complex terminal deposits containing elongated flowline patterns commonly emanate from the channel termini. These deposits could be composed of alluvial or hyperconcentrated flow sediments. The combination of smooth, lobate, and long, subparallel to interlocking delta plains within the same basin, with a third type, a very smooth deposit within the channel and its immediate terminal area (*e.g.*, Lake H1, Fig. 6) suggests that the basin floor may have had a variety of depositional settings and episodic activity. De Villiers *et al.* (2013) analyzed numerous types of delta forms on Mars, and concluded that they formed by *single* aqueous events, as suggested by the absence of fluvial modifications in both retrograding and prograding deltas. Our study shows that a single basin may contain several types and generations of deltas that suggest prolonged or repeated activity at the same site.

We find four instances where inlet channels did not enter the closed topographic basins but instead terminated at a small distance from them (basins H2, H3, NB6, and NB7; Fig. 4), and produced terminal deposits just outside the basin, which may be interpreted as subaerial delta plains (reflecting the terminal stage of delta development), or debris flow lobes, or alluvial fans from which water infiltrated and reemerged in the lake basin. H3 is a closed, circular basin, probably an ancient impact crater with a complex, layered deposit at $\sim$3 km distance from a fan-shaped terminal deposit (Fig. 7b). We interpret this intrabasin deposit as transported by the feeder channel into the basin, in multiple stages and modified by aeolian processes.

On Mars, we did not identify evidence for plunge pool morphology at channel entry points in the impact crater basins with significant drop of elevation from the crater rim. Instead, channels breach the crater rim with a long, deep valley section and terminate in a delta-like deposit (*e.g.*, through-flowing paleolake basins N6, N8; Fig. 4). We suggest that this morphology formed by back cutting, starting with a waterfall stage and developing further until the valley floor reached the base level of the lake. Similar canyons also represent base-level fall. Back cutting and absence of an apparent plunge pool suggest sustained, lower discharge flow and high sediment load in contrast to rapid flood scale turbulent flows that, for example in Dry Falls, Washington,

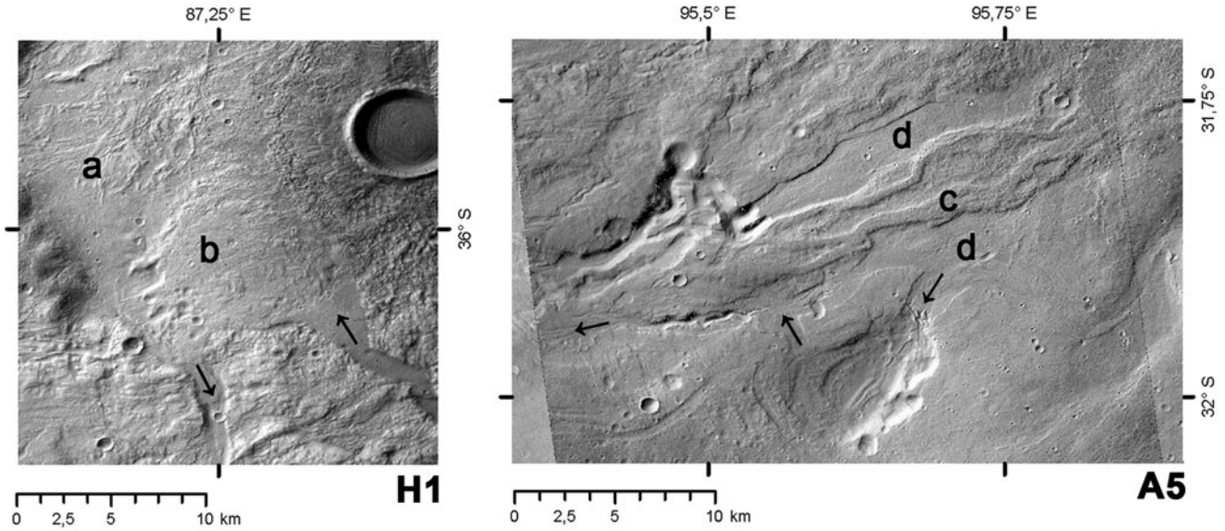

FIG. 6. Adjacent deposits of different types. **H1**, a: delta forms long ridges at the end of a long, discontinuous drainage, b: smooth-surfaced, Gilbert-type delta at the end of a short valley or channel filled with smooth deposit. Arrows show paleoflow directions. **A5**, c: inverted channels, d: normal channels. A5 is the basin in the middle.

produced plunge pools and potholes. A plunge pool may be buried under the terminal sediment or filled later. The outlet of N6 is also deeply incised. To activate this outlet, initially the entire basin must have been filled with water.

Alternatively, it may have formed by seepage at the outer side of the crater and slowly removed the crater rim by headward erosion of $\sim$5 km length. The terminal deposit of basin N8 is channelized in its entire length that suggests base-level fall during continued inflow.

5.3.2. Intrabasin deposits. We identified smooth interior deposits in 15% of the basins. Smooth interior deposits (*e.g.*, NB7) may be lacustrine, sedimentary, or aeolian in origin as they collected in local topographic lows. Typical flat, fine-grained deposits in terrestrial ephemeral lakes form playas (*e.g.*, Forester *et al.*, 2003). Approximately 32% of the basins have a LTD (*e.g.*, Mustard *et al.*, 2009; Wilson *et al.*, 2010; Wray *et al.*, 2011; Salese *et al.*, 2016) exposed on the floor adjacent to dark toned, in places pitted, latitude-dependent mantle (LDM). Long cliffs of LTDs may indicate lacustrine shorelines, or the existence of a former obstacle to LTD deposition. LTDs in the depressions of our mapping region are layered (basins N3, N10, and NB5) and are typically exposed at their frontal cliff margins. This suggests that mantling material was removed from the depression-facing slope margins, and these surfaces, including the cliff, are erosional, perhaps formed by coastal abrasion.

Typically, these exhuming LTD outcrops (Fig. 8) are scale like or polygonally fractured, suggesting desiccation processes. Remarkably, the frontal cliff of the N1 delta, the fan-like deposits (N2, N10, and NB5; Fig. 4), and also the nonterminal lake sediments (A2) all have a similar pattern. This suggests that LTD material in these paleolakes was sourced from flowing water, at different settings, and experienced similar cracking processes.

In A2, narrow, linear, interconnected ridges that we identify as Nili-type polygonal ridge networks (a type of feature initially described in Nili Fossae and Nilosyrtis regions by Kerber *et al.*, 2016) are situated on the top of LTD, which may be cemented subsurface fluid pathways. This large and deep depression may have experienced several lacustrine episodes compared with the others.

5.4. Ring of rough terrain

Some basins (N8, NB2b, NB2d, and NB7) exhibit a basin-marginal ring of rougher terrain that suggests periglacial processes operating beyond the immediate coastline. We found this morphology in 9% of the basins.

5.5. Lake "extensions"

Beyond the channel heads of Dao–Niger Valles, we have identified an $\sim$5 km wide elongated valley form with hanging walls protruding from the perimeters of two basins. The heads of the Peraea Cavus valley extension emerge at full length from the plains, at the northwestern side of the basin, close to Hadriaca Patera. We interpret these features as structurally controlled collapse valleys that may have been preserved from the initial stage of basin development. A similar feature is connected to Ausonia Cavus, which may have also functioned as an outflow channel to Niger Vallis.

5.6. Host features of the paleolakes

The host depressions of the candidate lakes are impact craters, erosional sub-basins in impact crater floors, steep-walled cavi, and rounded to oval topographic basins (see ''host'' column in Table 1). These topographic basins may have formed (1) in topographic lows enclosed by the front-lines of lobate impact crater ejecta and lava flows or wrinkle ridges, and represent a type of dammed lake; (2) in surface manifestations of buried and degraded Noachian impact craters; (3) in aeolian erosional depressions (blowouts); (4) in

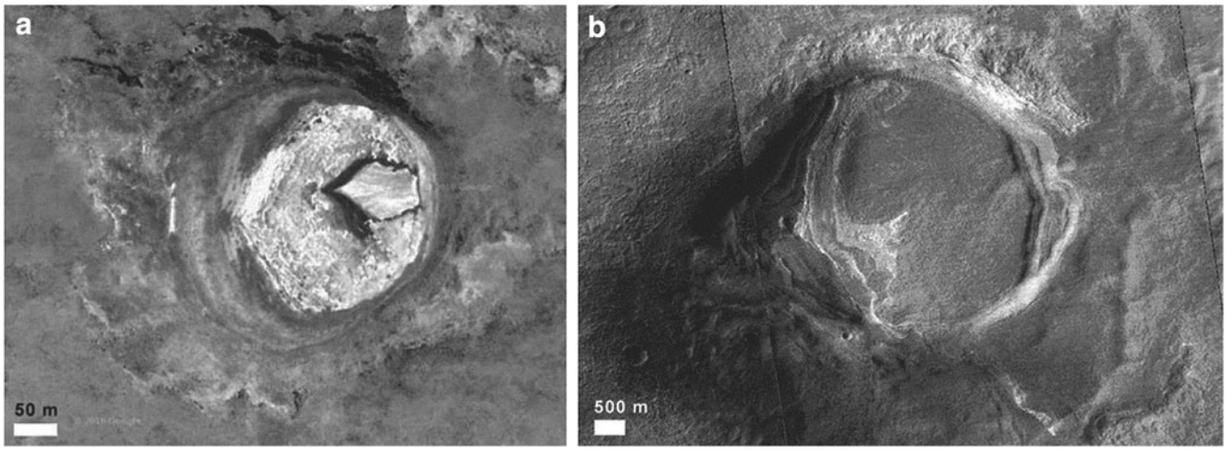

FIG. 7. Closed-basin lakes with layered deposits on Earth and Mars. The asymmetry of the martian lake could be caused by a feeder channel to the east, while the Patagonian lake's dry sediments are offset due to strong westerly winds. **(a)** Unnamed ephemeral lake in Patagonia, 48.35°S, 71.41°W, part of a group of similar lakes. Google Earth, Digital Globe. **(b)** Basin H3 at 36.5°S, 85.2°E, a channel-terminal depositional system on Mars (CTX mosaic).

depressions around which material was deposited at a time when a volatile or friable material filled these spaces; or (5) as random relief fluctuations in rolling terrain.

5.7. Terrestrial analogues

We present two terrestrial analogues. H3 is similar to closed-basin lakes in the cold semiarid climate Meseta Strobel basaltic plateau in Patagonia (Ariztegui *et al.*, 2010) (Fig. 7a). Another site in the high-elevation, arid Andes is in south Bolivia where Mars-analog volcanic and lacustrine (Fig. 9) features coexist. A group of ephemeral endorheic lakes lies adjacent to the Cerro Panizos ignimbrite shield that is surrounded by a deeply dissected ash apron (Greeley, 1994:54), showing similar morphology to Tyrrhena and Hadriaca Montes. When dry, these basins are covered by saline crust over lacustrine sediments. Solutes are accumulated by volcanic hydrothermal circulation and ash fall and are transported into the salars through groundwater seepage (Fig. 9). Flash floods provide ephemeral fluvial input for the dry salars, while wet salars (perennial brine lakes) are fed by longer, perennial streams. Feeder channels deposit alluvial fans (Fig. 9j). Salars are filled by clasitcs and evaporites (Ericksen, 1987; Warren, 2016:265).

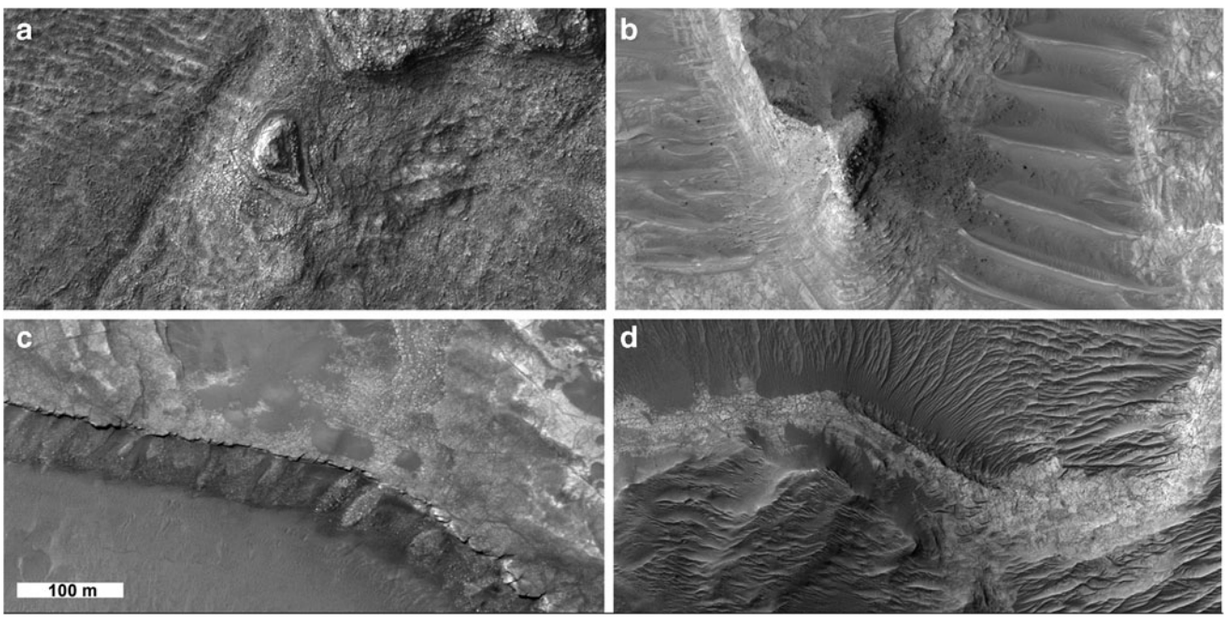

FIG. 8. Outcrops of light-toned layered deposits in candidate paleolakes. **(a)** streamlined (aeolian?) form in NB5 paleolake in Majuro crater, **(b)** layered mesa in A2, Peraea Cavus, benches are 4 m wide, **(c)** fan cliff in N10, **(d)** delta front in N1. All deposits show 1–4 m diameter fractures. HiRISE images **(a)** PSP_009151_1465, **(b)** ESP_021717_1500, **(c)** ESP_040601_1460, and **(d)** PSP_001820_1520.

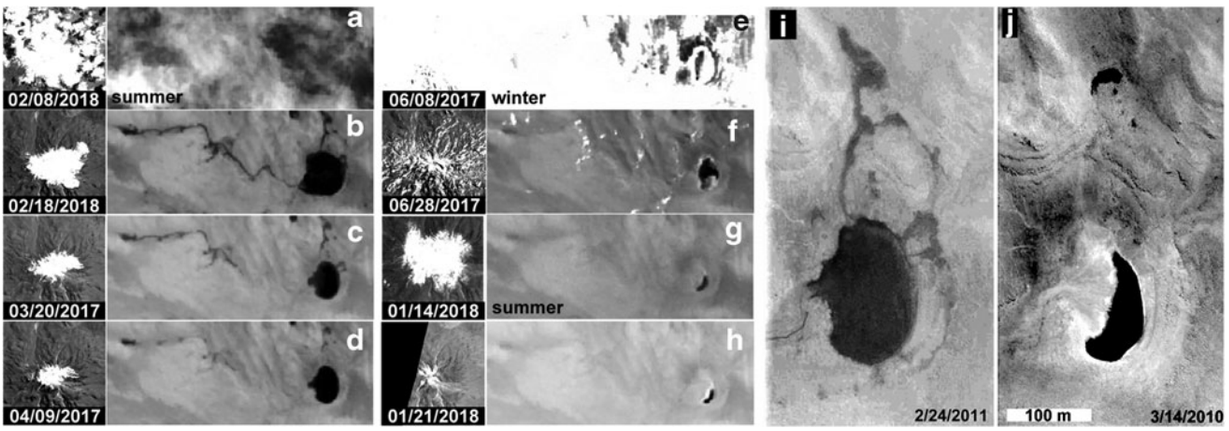

FIG. 9. Seasonal changes in a terrestrial analog ephemeral lake, in Bolivia. Left panels show the top of the adjacent Uturuncu volcano. **(a–h)**: progress of lake water discharge over the course of a year. Lake recharge occurs during the rainy summer **(a)** when the top of Uturuncu receives snow. While the snowcap decreases **(a–d)**, shorter seepage channels slowly recede and eventually dry up. A winter snowfall **(e)** does not increase water levels, and lake surfaces freeze. An isolated snowfall at the top of the volcano does not increase lake water level **(g)**. The lake almost entirely dries up **(h)** by the time the next rainy season arrives (2017–2018, 10 m/px Senitel 2 images); **(i)** groundwater seepage from cliffs in the layered substrate reaches the refilled lake (corresponds to **c**); **(j)** large alluvial fan produced by inlet channel to the west is apparent at low water level with bright deposits at its lake side margin (corresponds to **g**); (**i–j**): High-resolution Google Earth/Digital Globe images centered 22.263°S, 67.011°E, Earth. Note similarities of **j** and **i** to N10 low and high stand extents.

The patterns of bright deposit-covered margins underlying alluvial fans are similar to LTD outcrops at the margin of fan-shaped deposits (A2, H2, N3, NB5, and N10) at the margin of paleolake basins. Single seepage input channels may be analogous to short, single inlets (*e.g.*, NB2a), while the longer channels on Mars are more similar to perennial feeder channels on Earth. However, in Bolivia, the terrain around the lake basins is not sloping, and there are no outlet channels. Smaller lakes that dry up first are few tens of meters higher than larger lakes that are at similar elevations.

6. Paleolake Volumes

6.1. Methods

We measure ancient water volume within the basin areas by finding the difference between the paleolake surface level and MOLA topography. In ArcGIS, we produced polygons of paleolake basin extents following elevation contours and morphological cues, extracted interpolated MOLA MEGDR (Smith *et al.*, 2003) elevation contours, and then used the Surface Volume tool to compute the volume between the MOLA elevation contour and the potential paleolake terrain. Although additional editing techniques may introduce small errors, the difference product may be improved in quality for complex terrains. For example, when searching for paleolake volumes of a basin whose margin has been obscured or eroded by more recent processes, it may be useful to reconstruct the break by interpolating prebreak surface. We restored one such ridge (Basin N11, Fig. 4) that was likely breached at the end of Navua A to determine bank full volumes before the putative breach.

6.2. Results

Lake volumes range from 0.02 to 1055 km^3. The total maximum paleolake water volume contained here in this mapping region is 2667 km^3, nearly as great as the water volume within Lake Victoria on Earth (2700 km^3). These values are comparable with volumes generated from the multiplication of average depth by area. The average area covered by these potential water bodies is $\sim$351 km^2 with the average diameter of 23 km, and the average depth is 74 m. The average depth of open and closed paleolakes is similar, 81 and 48 m, respectively. Table 1 shows volume and depth data of each candidate paleolake. The largest volumes within a single group may be used as an estimate of the minimum volume of water present in the system.

7. Paleolake Floor Ages

7.1. Previous work

Valley network formation (Gulick 2001) is constrained to the period near the Noachian–Hesperian boundary (3.8–3.6 Ga) (Hoke *et al.*, 2011). Wilson *et al.* (2016) identified fresh shallow valley and chain lake systems formed near the Hesperian–Amazonian boundary. However, lakes could have continued to form by periglacial (Soare *et al.*, 2008) or glacial (Di Achille and Ori, 2008) processes during the late Amazonian.

Beside global climate changes, local conditions controlled by the Tyrrhenus–Hadriacus volcanic complex include the mobilization of subsurface volatiles, and degassing that may have contributed to localized precipitation near the volcanic centers. The closest caldera, Hadriaca Patera, formed at 3.5–3.6 Ga (Williams *et al.*, 2007; Werner, 2009; Robbins *et al.*, 2011) and resurfaced at 2.6 and ultimately at 1.5 Ga when its southern flanks were fluvially dissected (Gulick and Baker, 1990; Williams *et al.*, 2007), marking potential events that could have initiated lacustrine developments.

7.2. Methods

We have calculated formation and resurfacing ages of each basin using crater counting techniques. We have

included the entire area within the putative MOLA-based lake boundaries as a single unit, except where a bench and outlet/inlet channels were situated at different heights. In these settings, we introduced a low stand and a high stand lake size. Given that we considered crater diameters <120 m, these small crater sizes could introduce potential error from secondary contamination. However, potentially differing crater retention ages of deltas, exposed and possibly exhumed LTDs and crater floors may have resulted in additional errors.

We used Hartman and Neukum's (2011) chronology function, and Ivanov's (2001) production function. Crater statistics were recorded with CraterTools in ArcMap (Kneissl *et al.*, 2011), and size–frequency distributions (Neukum *et al.*, 2001) were analyzed with CraterStats II software (Michael and Neukum, 2010; Michael *et al.*, 2012) using isochron-fitting technique to derive model crater ages. We counted all craters at CTX resolution (down to $\sim$15 m diameters) and excluded groups of secondaries. For Ausonia Cavus (Basin A6), which was partially beyond our mapping area, we used crater counting ages from Musiol *et al.* (2011).

We have tested whether the sizes of crater counting areas influenced the results. Areas and formation ages had a weak positive correlation of $r = 0.36$. We excluded the four extremes—the largest area (NB3, 3.85 Ga) site, two sites with the youngest ages and also the smallest areas (A5 and H3 smaller than 30 km^2) and NB2b (part of a group with typically older ages), all marked very uncertain in Table 5.

Table 5. Crater Counting Results

Name	*Lake, area, km²*	N	D_{min}	D_{max}	*N(1) 10^{-5} km^{-2}*	*Age*	*Err+*	*Err–*	*Confidence*
A1	230	17	500	700	649	3.71	0.04	0.06	Good
A2H	391	4	400	450	53	1.11	0.49	0.49	Uncertain
A2L	928	49	200	400	49	1.02	0.13	0.13	Good
A2L	928	5	800	1500	293	3.51	0.1	0.36	Good
A3	277	33	250	400	116	2.37	0.36	0.37	Good
A3	277	5	600	800	321	3.54	0.1	0.29	Good
A4	363	87	150	300	49	1.02	0.1	0.1	Good
A4	363	3	500	700	238	3.44	–0.13	0.72	Good
A5	26	3	170	250	13	0.283	0.16	0.16	Very uncertain
A6						3.71*			Musiol *et al.*
A6						1.85*			Musiol *et al.*
H1	313	14	300	450	150	3.01	0.27	0.61	Good
H1	313	2	700	900	345	3.56	0.11	0.59	Good
H2	102	10	200	250	49	1	0.26	0.26	Good
H2	102	3	450	700	240	3.44	0.15	1.3	Good
H3	29	1	120	120	2.2	0.045	0.045	0.045	Very uncertain
N1	314	33	500	900	308	3.53	0.04	0.05	Good
N1	314	7	1100	1500	850	3.76	0.04	0.06	Good
N1	314	4	3000	7000	1950	3.9	0.06	0.11	Good
N2	262	41	170	250	32	0.661	0.09	0.09	Good
N2	262	3	450	500	137	2.79	0.53	1.1	Uncertain
N2	262	3	800	1200	802	3.75	0.08	0.19	Good
N3H	829	36	250	400	40	0.831	0.12	0.12	Good
N3H	829	3	800	3500	307	3.53	0.11	0.46	Good
N3 L	478	6	400	500	66	1.37	0.5	0.5	Uncertain
N4	235	16	300	500	55	1.13	0.28	0.28	Good
N5	249	25	170	300	20	0.409	0.074	0.074	Good
N5	249	3	400	500	67	1.38	0.68	0.68	Good
N5	249	1	1300	1300	891	3.77	0.12	3.6	Uncertain
N6	258	24	421	1320	415	3.61	0.04	0.06	Good
N7	40	2	450	700	407	3.61	0.11	1.1	Uncertain
N-A1	37	9	150	200	48	0.999	0.3	0.3	Uncertain
N-A1	37	2	350	500	156	3.08	0.4	2.1	Uncertain
NB1	105 (55**)	9	200	450	105	2.15	0.69	0.71	Good
NB1	105 (55**)	32	130	170	51	1.05	0.15	0.15	Good
NB2b	46	17	140	250	23	0.484	0.12	0.12	Very uncertain
NB2c	105	34	120	170	34	0.521	0.073	0.073	Good
NB2c	105	10	200	400	67	1.37	0.43	0.43	Uncertain
NB3	1461	50	400	900	150	3.03	0.19	0.35	Good
NB3	1461	2	2000	3500	1450	3.85	0.09	0.23	Good
NB8	128	20	170	300	36	0.74	0.14	0.14	Good
NB8	128	4	400	600	240	3.22	0.2	1.2	Good

Depressions with very uncertain results are excluded. Age of A6* is from Musiol *et al.* (2011). *Basin age results are very uncertain likely because it combines different units. Ages of depressions in the same drainage upstream are given instead. Ages calculated using the Hartman and Neukum (2011) chronology function. Two asterisks (**) indicate the actually measured area. N is the number of craters used in the measurement, D_{min} and D_{max} are the diameters of the smallest and largest craters in the measurement. N(1) values show the density of craters with diameters (D) ≥1 km per km^2.

Excluding these, correlation between age and counting area became negligible ($r = 0.07$).

7.3. Results

We could determine the ages of 21 candidate paleolake depressions (Table 5). Their calculated ages (resurfacing and formation) concentrate in the periods 3.75, 3.54, 1.37, 1.00, and 0.5 Ga. Isolated age values are scattered between 3.2 and 2.1 Ga. Formation ages concentrate $\sim 3.5 \pm 0.4$b Ga (Hesperian) for 14 depressions, with one depression at 2.1, two at 1.11, and two at 1.37 Ga (Fig. 10).

We could not find a consistent fit in the other depressions' crater data, which may be due to several reasons, including strata of multiple ages, different exposure times, erosion histories, very high ratio of secondaries, or very small counting area.

The oldest crater retention ages of the depression surfaces are similar to the age of the valley networks on Mars, which is consistent with an aqueous episode in the depressions.

The 3.54 and 1.00 Ga surface ages can be traced throughout the entire Navua, Hadriacus, and Ausonia regions, which suggests that the conditions in these regions at those times were likely similar. The 3.54 Ga age is consistent with the formation of Hadriaca Patera, and any lakes of this age were likely supported by hydrothermal systems from volcanic heating (Gulick and Baker, 1990; Gulick, 1998). Two paleolake floors along a branch of the Navua A drainage are dated 3.6 Ga, which is contemporaneous with the material of the plains into which Navua A is incised (Hargitai *et al.*, 2018). This suggests that the materials on the lake floors are either not lacustrine, or the lacustrine layer is insignificant and cannot be detected by crater counting.

Alternatively, the similar age of a paleolake floor and the surrounding terrain may suggest that the paleolake formed shortly after the plains-forming material. Therefore, the Navua A channels and the formation of lakes are contemporaneous. The interior and exterior deposits of Ausonia Cavi are similarly contemporaneous (Musiol *et al.*, 2011).

The depressions resurfaced at 1.00 and 0.5 Ga ago, after volcanic activity had stopped at Hadriaca Patera. Therefore, these episodes were likely decoupled from volcanic heating and represent localized Amazonian processes.

Our crater counting suggests that the lakes in the NHA region formed during the same broad period as lacustrine sediments were deposited in Terby crater (Wilson *et al.*, 2007), in Hellas, and other paleolakes (Fassett and Head, 2008), isolated in time and space. The NHA region's lakes represent a late activity within this period, probably linked to volcanic activity in the Hadriacus Mons region, which

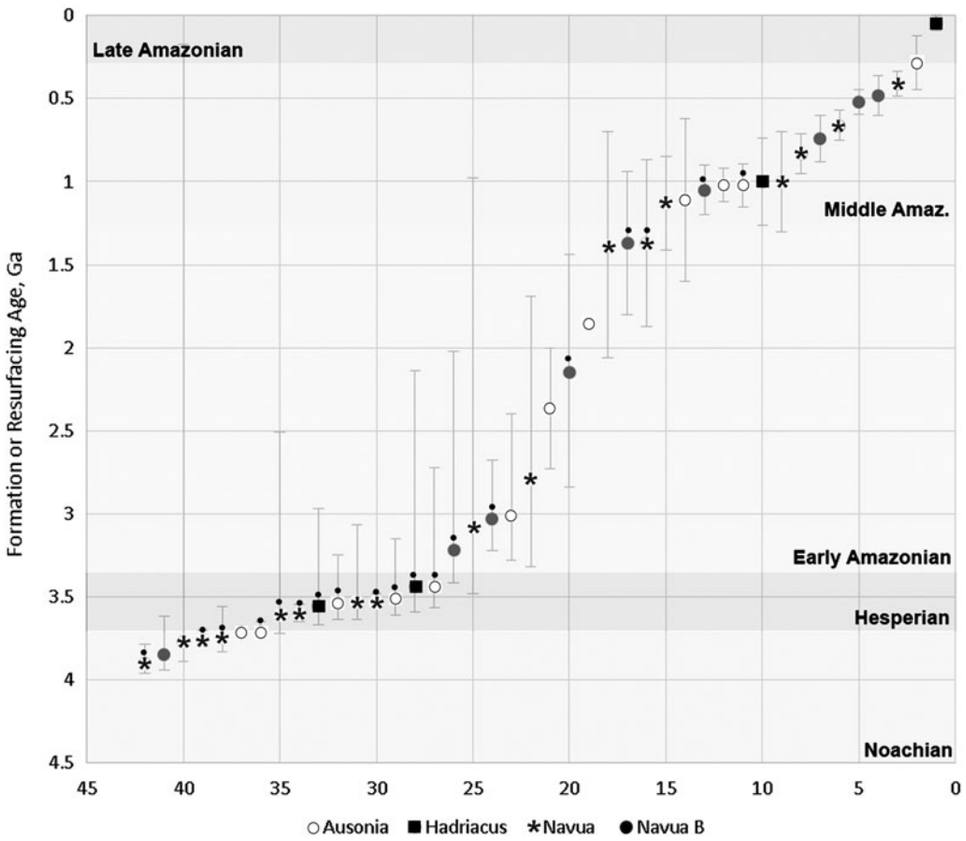

FIG. 10. Crater retention ages of all 42 measurement points, in 21 of the candidate paleolake basins, arranged in decreasing age, in the Navua–Hadriacus–Ausonia Region, Mars. Flat ''surfaces'' show periods when several surfaces formed or resurfaced at the same time. Period and epoch boundaries are based on Hartmann and Neukum (2001). Small black dots indicate unit formation ages, undotted ages are resurfacing ages.

Table 6. Ages of Fan-Shaped Deposits

Name	*Lake, area, km²*	N	D_{min}	D_{max}	N(1) 10^{-5} km^{-2}	*Age*	*Err+*	*Err−*	*Confidence*	*Host, basin age*
H1 upper deposit	92	11	300	500	155	3.06	0.28	0.84	Uncertain	3.01, 3.56
N2b deposit	6	4	130	150	29	0.68	0.3	0.3	Uncertain	0.484
N11 deposit	117	2	282	500	700	3.5	0.14	1.8	Uncertain	3.6, 1.1-1.3*
N11 deposit	117	7	66	200	400	1.37	0.45	0.45	Uncertain	

*Basin age results are very uncertain likely because it combines different units. Ages of depressions in the same drainage upstream are given instead. Ages calculated using the Hartman and Neukum (2011) chronology function. N is the number of craters used in the measurement, D_{min} and D_{max} are the diameters of the smallest and largest craters in the measurement. N(1) values show the density of craters with diameters (D) ≥1 km per km^2.

also generated localized precipitation in the Navua Valles head region (Hargitai *et al.*, 2017).

7.3.1. Ages of fan-shaped deposit. We considered the possibility that the lake surfaces we dated significantly predate the terminal deposit surfaces, which would suggest that the deposition of the delta-shaped sediments did not coincide with a basin-wide deposition event, and that the horizontal strata are volcanic or aeolian materials. We have selected the largest delta-like deposits of which four resulted in consistent crater size–frequency curves. The ages of the deposits are largely within the error bars of the ages of the host basins (Table 6), in both Hesperian and Amazonian surfaces. Stratigraphic relations suggest that the terminal deposits postdate the formation of the basin floor and formed soon after the lake floor deposits.

8. Groups of Putative Paleolake Depressions

We have grouped spatially associated paleolake basins, and found that they share similar characteristics:

8.1. Upper Navua A Crater Lakes

This group (Fig. 11) includes four adjacent impact craters (N2, 3, 4) that were probably exposed to precipitation. A nearby fifth crater (N1) contains a short, integrated valley system that probably transported water out of this area. The morphologies in the putatively precipitation-fed craters include a dissected crater rim, fan-shaped deposits with narrow channels, and crater interior delta, typically with short inlet valleys. These craters are concentrated in the upper Navua A region. We interpret this region as one that likely received significant precipitation, which could have supported closed lakes and dendritic streams.

This region is also abundant in valleys and channels whose floors exhibit few decameter-sized mounds or knobs. Their morphology is consistent with pingo, spring mound, fumarolic mound, or mud volcano origin. Knobs postdate channels that support pingo and not spring mound interpretations, since spring mounds should be contemporaneous with the presence of surface water and pingos, are produced from subsurface water processes in permafrost. Knobby channels and basins have been identified in several different regions on Mars (Hargitai and Gulick, 2018), which suggests that their formation is more likely related to climatic rather than volcanic processes. The region around crater N3 is the only area in the Hadriacus region, where precipitation was likely, as implied by the dense integrated drainage networks, unlike in other places in the Navua region where drainage is subparallel or characterized by single channels not connected to drainage divides (Hargitai *et al.*, 2017). The model of meteoritic rain or snowmelt origin is consistent with that of the crater lakes in the region.

The area of N1–N5 craters is the only place in our mapped region where impact crater lakes occur without inlet valleys and still show several paleolake indicators, including deltas, interior channels, fan-shaped deposits, cliffs, benches, and incised crater walls. Valleys formed on both the interior and exterior rims of these craters but did not breach crater rims.

The largest crater lake on the northern edge of this area is adjacent to integrated valley networks, but probably received little direct precipitation as its crater walls are not incised. The upper Navua A highland area, which likely received precipitation, is $\sim 160 \times 150$ km large. Craters mapped elsewhere in the region either show no morphologies that would indicate paleolake formation or where they do, they are clearly fed by an inlet channel. The only exception to this is Majuro crater, which also has heavily incised crater walls yet possesses no inlet channel. A large channel suggests that groundwater flow processes were active, because it dissects the Majuro crater ejecta and widens proximal to this crater without developing any tributaries from the crater wall (Hargitai *et al.*, 2017).

Paleolake bed surfaces in the Upper Navua A craters show crater counting formation ages 3.7–3.5, 1.4–1.1 Ga, and a relatively recent resurfacing age at 0.8–0.4 Ga. These events were limited to different combinations of craters, where the Hesperian event affected the northern craters, the earlier Amazonian event affected only the southern craters, and the later Amazonian event affected both groups. Knobby terrain formation in this region is the uppermost stratigraphically and may be related to the last Amazonian resurfacing event. Intracrater features are likely related to different events, as the now degraded crater wall valleys were incised during earlier events, the pristine-appearing fan-top channels and cliffs of LTDs formed or exhumed in the later (younger) episode.

8.2. Upper Navua B Lake Group

Both branches of Navua B emerge from depressions, which we interpret as dominantly groundwater-fed lakes (Fig. 12). The eastern branch originates from a group of depressions, some of which are connected while others have no apparent surface outlets. The maximum depth of water of the NB2 group is 55 m, whereas the overall average depth is 13 m.

Unlike Navua A, which is closer to the highlands, Navua B is closer to the Hadriacus volcanic center, which may have

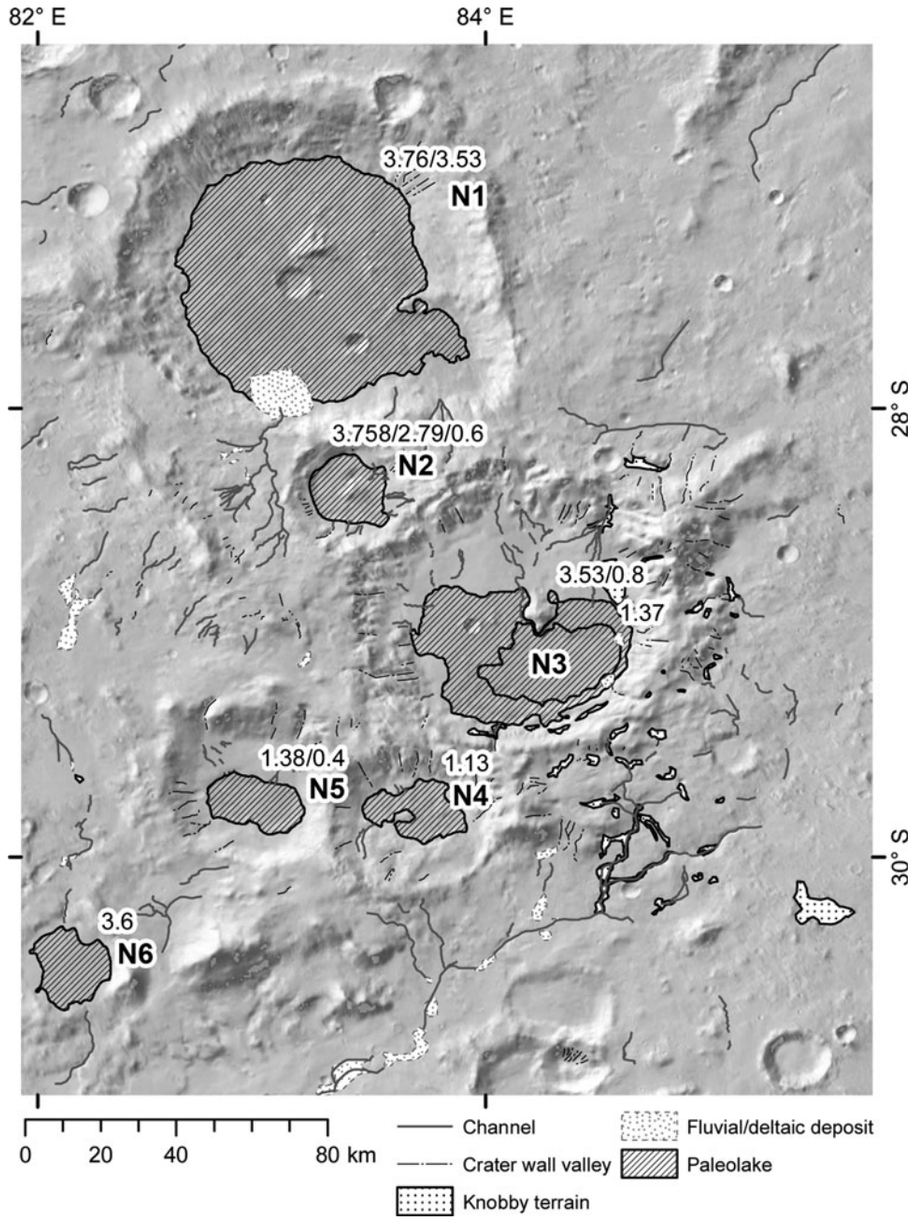

FIG. 11. Putative paleolakes at the source of Navua A. Numbers show crater retention ages. See Figure 3 for legend. Labels show paleolake IDs.

been fed by lakes. These are the only potential lake depressions in the region that exhibit knobby terrain, which might indicate the presence of abundant groundwater, if these knobs are interpreted as either pingos or spring mounds. Both branches terminate in another, large paleolake basin with knobby terrain (NB3). This lower, large depression formed in the Noachian and resurfaced in the Early Amazonian, while the surfaces of the source basins connected to the two upper branches are dated Amazonian. This suggests that these branches were not present when Navua B originally formed, and so they might not have played a role in the lower paleolake's formation. Nearby craters and peaks with incised slopes suggest local precipitation, which may have fed that lower paleolake.

However, this would have been significantly less precipitation than in the Navua A source region, as integrated valleys did not form.

8.3. The Ausonia Lake Chain

8.3.1. Description. The Ausonia paleolakes (Fig. 13) are a chain of depressions located at different elevations and are connected by narrow channels and wide and subdued valleys. The depressions include steep-walled cavi and gently sloping basins. This system is the most proximal to the Hadriacus volcanic center and is located at the head of a major outflow channel system. Basin A2 exhibits a 5 km wide, elongated valley form. Depressions at the lower end of

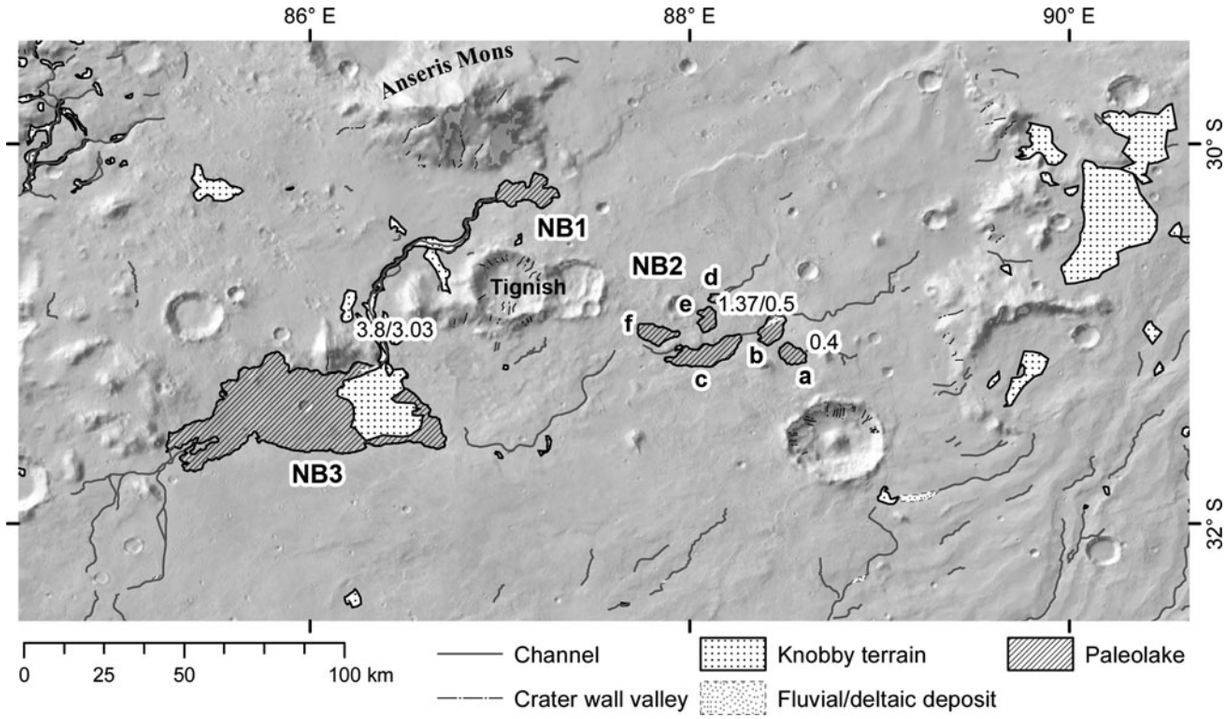

FIG. 12. Depressions (blue) in the source region of Navua B. Anseris Mons, a nonvolcanic peak with a southern steep scarp (red line), is dissected only on its southern, pole-facing side. See Figure 4 for legend. Background: MOLA shaded relief.

the system include adjacent braided-inverted and regular channels (north of A5, Fig. 6), where the inverted channel may be fluvial or volcanic, with long period between the channel-forming episodes. These lakes have the same crater ages as the other lake groups: 3.7, 3.5, and 1.0–1.1 with resurfacing events scattered between 1.8 and 3.0.

A discontinuous fluvial pathway can be traced 300 km upstream of these lakes, which suggests that they may have received water from upslope through subsurface currents.

Lake depressions are progressively younger downslope from the highlands to the outflow channels. Peraea Cavus, closest to Hadriaca Patera, in the middle of the Ausonia-lake-chain system, formed at the same time as Hadriaca Patera. This suggests a downslope migration of lake-fluvial system development, likely controlled by volcanic processes.

The regional lava plains have similar histories (formation at 3.7 Ga, resurfacing at 1.8 Ga, Musiol *et al.*, 2011), which suggests that volcanic events significantly contributed to the formation of the depressions or of their floor materials; however, some of the depressions formed hundreds of millions of years later. These systems may have continued to provide habitable environments after the volcanic activity ceased.

8.3.2. Previous mapping, interpretation. Crown and Greeley (2007) geologically mapped this area at 1:1 M Scale, at a significantly smaller scale than our mapping. At that scale they failed to identify the topographic basins as separate geological units, did not connect the two cavi, and did not map any channels north of Peraea Cavus. However, we mapped several sections of a discontinuous channel system through Savich crater. Crown and Greeley (2007) interpreted the two cavi as collapse depressions in water- or ice-rich materials. They interpreted their floors as sedimentary deposits similar to those, and part of, Dao and Niger Vallis, and dated them Late Hesperian to Early Amazonian.

Bernhardt *et al.* (2016) interpreted the cavi as outflow channels carved by extensive groundwater sapping mobilized by volcanic heat. Musiol *et al.* (2011) proposed that volcanic loading around Hadriaca Patera caused tensional fractures, which evolved into faults and acted as flow conduits for overpressurized groundwater. This overpressurized groundwater flow caused collapse in several source regions, and multiple outflow and recharge events.

Similar interpretation is proposed for troughs in Noctis Labyrinthus, which are shallower than that in Peraea Cavus. Rodriguez *et al.* (2016) examined the Noctis area and suggested that the orientation of troughs represents structurally controlled groundwater flow paths. Similar flow paths may have caused the nearby, much smaller scale, sinuous pit chain features on the southern base of Hadriacus Mons (Crown *et al.*, 2005), which are, however, absent in this northern part.

A similar feature, Ismenius Cavus, associated with channels and terminal deposits, was proposed to be a 600 m-deep paleolake (Dehouck *et al.*, 2010). Based on this analogy, Hamilton *et al.* (2015) suggested that Peraea and Ausonia Cavi may have also been paleolakes and proposed this area to be a candidate landing site for human Mars missions. Di Achille and Ori (2008) also interpreted a similar, steep-sided, rounded-oval feature in Arabia Terra as paleolake.

However, we interpret the basin valley forms as faults resulting from stresses caused by Hadriaca Patera and outflow

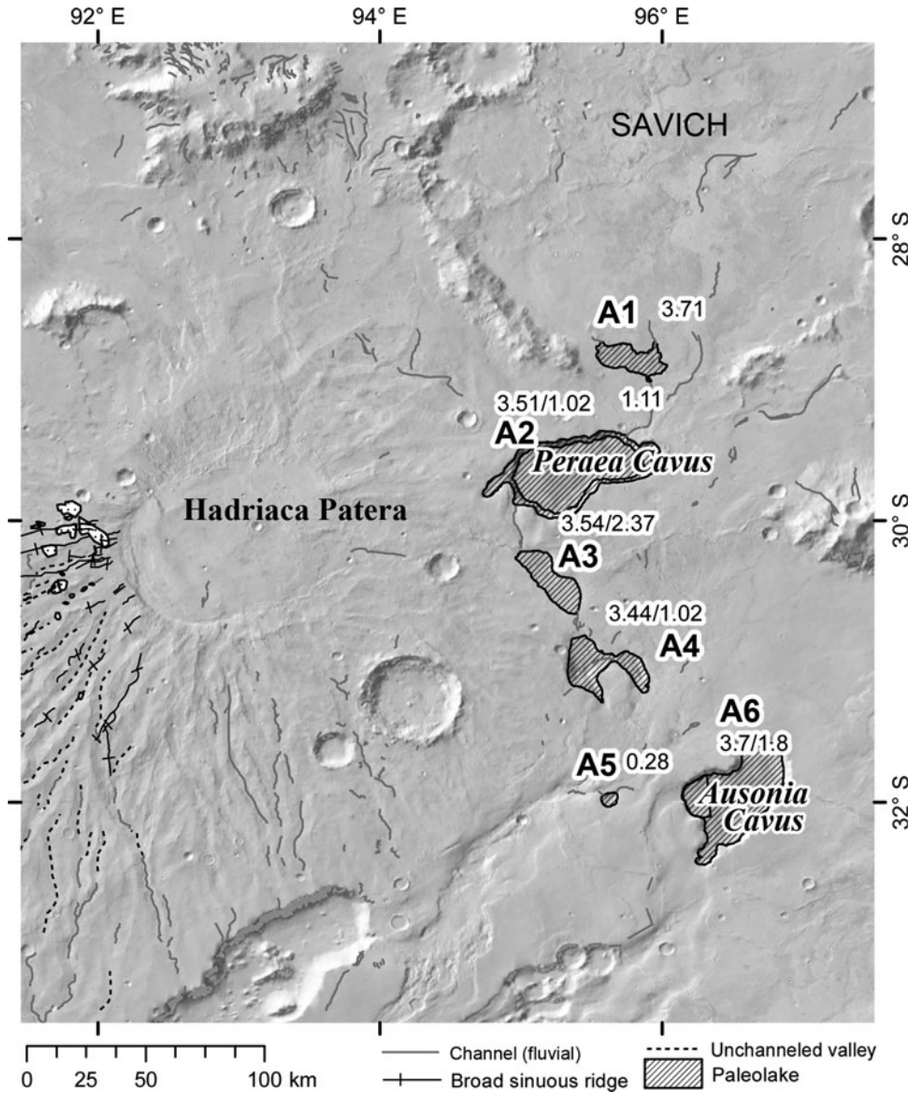

FIG. 13. The Ausonia Region paleolakes East of Hadriaca Patera. Background: THEMIS day IR mosaic.

of overpressurized groundwater mobilized due to volcanic heat. While these cavi may have formed by collapse, they are not directly connected to outflow channels like other channels associated with chaotic terrain. This suggests that water was kept in Peraea Cavus after the collapse, but the lower basin, Ausonia Cavus, does have two wide hanging outlets.

Narrow inlet and outlet channels suggest that surface runoff also contributed to the draining and formation of the paleolakes in these basins. As shown in Figure 11, our mapping of the channel segments and flow paths shows that the main surface water contribution was received from the northeast through Savich crater, and not from Hadriaca Patera.

8.4. Other lakes

Terminal and through-flowing lakes scattered in the region are here identified as fluvial-fed lakes. The origin of these depressions is either impact related, or by enclosure of ridges or flow fronts.

We identify two concentrations of lakes in this group: one where Navua A and nearby channels terminate in Hellas Basin (Fig. 14a), and another around Poti crater (Fig. 14b) whose walls are dissected by fresh-appearing linear gullies.

N10 is an example of a through-flowing lake (Fig. 15). This lake is one of the ''Hellas Group'' lakes listed by Cabrol and Grin (2001) that experienced ''short ponding possibly associated with limited hydrothermal activity.'' This basin is situated in Crater 28-76 (Crater ID from Robbins and Hynek, 2012), and is connected to a major drainage of the Navua Valles, informally called Navua A (Hargitai *et al.*, 2017). This crater is also listed in Fassett and Head (2008) and in Goudge *et al.* (2012) as open-basin lake No. 128, containing a delta deposit. Similar, degraded, and smooth deposit filled craters in the Reull Vallis plains are, however, interpreted to be *exhumed fluvially* (Mest and Crown, 2001). In Crater 28–76, at CTX resolution, the fan-shaped terminal part of the channel appears to be erosional, similar to an estuary.

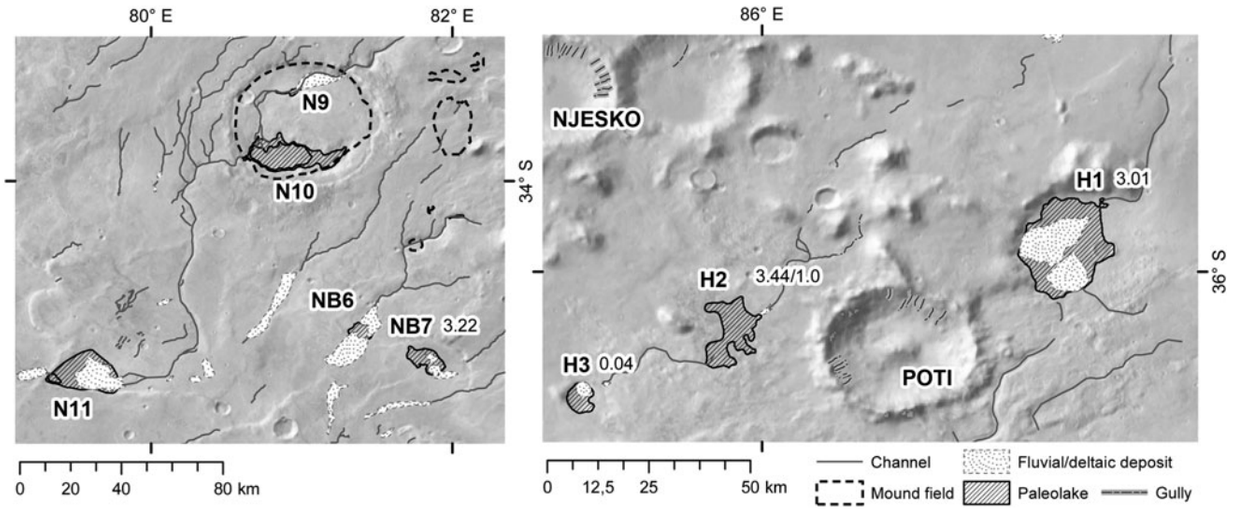

FIG. 14. Two groups of lakes, left **(a)**: lower Navua A, right **(b)**: near Poti crater. Labels show the putative paleolake IDs used in this study (Fig. 1). Orange lines show mound field surfaces.

8.5. Sources of water

The lakes we described are concentrated in five locations (Table 7): upper Navua A, lower Navua A, upper Navua B, Ausonia, and at the foot of Hadriacus Mons around Poti crater. The Navua A lakes are likely related: water in the upper Navua lakes were collected from the same source, likely precipitation, that formed the Navua A channels; middle and lower Navua A lakes formed at intermediate and final termini of these surface water pathways. Upper Navua B lakes are related to these channels, but they are at various positions: source, intermediate, terminal, and independent, which suggests that a localized event, perhaps glacial melt, provided groundwater to fill these depressions. Craters in the

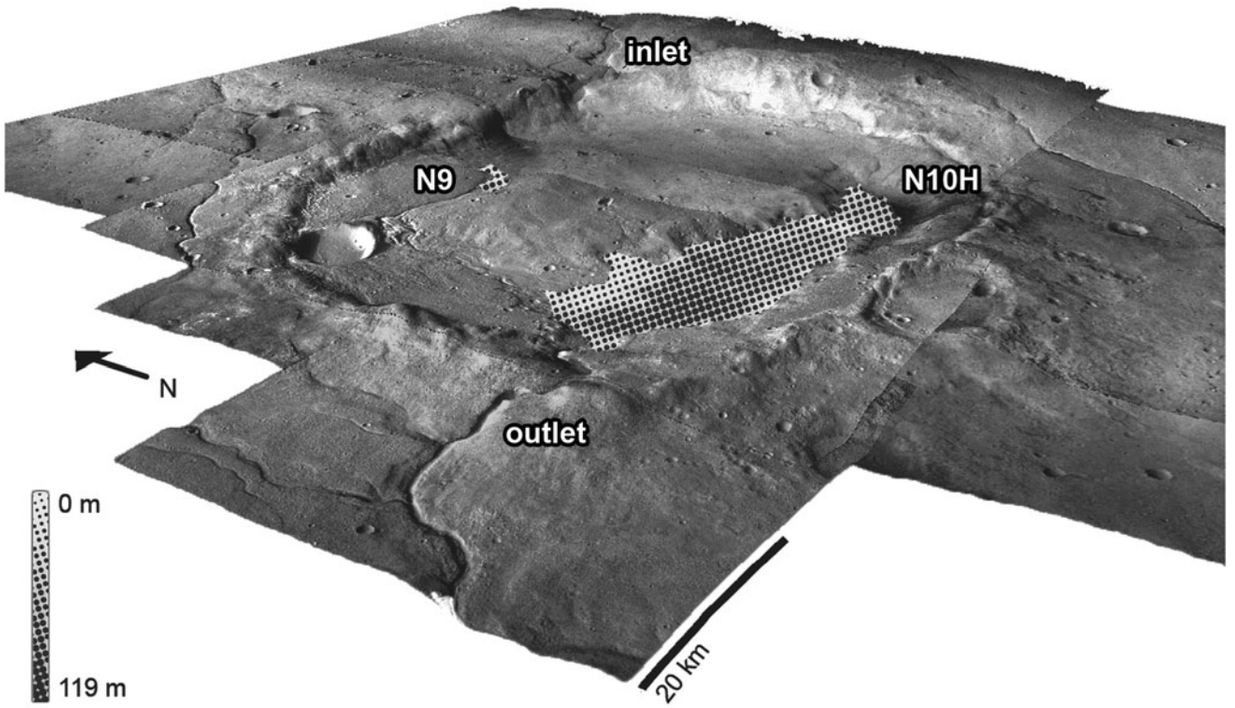

FIG. 15. 3D perspective view (CTX mosaic over MOLA, 5× vertical exaggeration) of minimum fill volume difference raster for crater sub-basin paleolakes N10H and N9. Sizes of dots indicate water depth. A small and narrow valley dissects the interior deposit near label N10H.

Table 7. Dominant Characteristics of the Five Lake Groups in the Navua Valles–Hadriacus Mons–Ausonia Montes Region

Group	*Source (primary, secondary)*	*Dominant paleolake types*
Upper Navua A	Precipitation	Closed impact crater lakes
Upper Navua B	Precipitation, groundwater	Topographic source lakes
Lower Navua A	Surface water pathways, groundwater	Topographic terminal lakes
Ausonia	Volcanic mobilization of ground ice/liquid water	Through-flowing cavi lakes
Near Poti	Volcanic mobilization of ground ice/liquid water	Various

vicinity of these lakes are gullied, which may be related to the same groundwater or snowmelt. Poti crater, near the Hadriacus–Poti lakes, is likewise gullied, with unusually fresh morphologies.

Groundwater-sourced lakes are all at the foot of Hadriacus Mons that suggests that they are related to volcanic activity, for example, mobilization of ground ice, while precipitation-fed Navua A lakes are further away. These lake groups are, therefore, morphological manifestations of isolated sources and/or localized mobilizations of subsurface or surface water, some of which were collected or emerged at the location of the lakes, others upslope of them.

9. Habitability Assessment

Favorable habitable conditions could have been provided in lakes closest to a thermal source. Such heat sources may be impact related (Daubar and Kring, 2001; Kreslavsky and Head, 2002; Osinski *et al.*, 2013) or volcanic (Gulick and Baker, 1990; Gulick, 1998), the latter of which could be Hadriaca and Tyrrhena Paterae in this region. Volcanism, unlike a single impact thermal event, could be reactivated repeatedly by an extensive subsurface dike system or by multiple episodes of magma entering into the magma chamber. Fault systems may also act as conduits for fluids, and so heated groundwater flowing into lake systems along fault lines connecting to either recent impact or the volcanic centers may increase habitability potential.

The closest depressions to Hadriaca Patera (such as lake A2, Figs. 4 and 11) formed 3.54–3.51 Ga ago, which is consistent with the formation of Hadriaca Patera. If the lake extensions such as the one at lake A2 are such conduits, then this lake would have the highest astrobiological significance where water, nutrients, and heat source were equally available. Life could have been sustained for prolonged period in subsurface voids similar to isolated terrestrial subsurface fracture habitats (Chivian *et al.*, 2008). The calculated water depths (Table 1) could have provided shielding from harmful cosmic and UV radiation in the water and at the lake floors.

All lakes in the NHA region of northeast Hellas had active periods throughout the Noachian, Hesperian, and Amazonian time periods, which should be favorable for habitability. Despite the potential for prolonged periods of inactivity, alluvial, deltaic, and lacustrine deposits would preserve records of paleoclimate, paleoenvironment, and habitability.

10. Conclusion

We have mapped potential paleolakes in the Navua–Hadriacus–Ausonia region, northeast of Hellas Basin, building on our previous drainage mapping. We have identified 34 depressions that potentially hosted paleolakes, which would have contained >2600 km^3 of water. Some of these depressions we classify into groups that likely had individual origins.

We have identified a group of crater lakes likely fed by meteoritic precipitation, a group of basins likely filled by groundwater, and another group that likely formed by a combination of tectonic stresses and overpressurized groundwater flow. The rest of the putative paleolakes scattered in the region were surface water or groundwater fed. Crater retention ages of the depressions suggest that some formed during a volcanically active period in the Hesperian when highland valley networks and related lakes were also produced elsewhere on Mars. These depressions were resurfaced, and some formed after volcanic activity ceased in this region during the Amazonian. This suggests that these lakes may have had multiple resurfacing episodes, and during these episodes they may have received water from different sources. Lakes may be related to gullies because they tend to occur at the vicinities of gullied craters.

Concentration of lakes into groups suggests that water was collected or mobilized at isolated locations. The lakes that formed in proximity to Hadriaca Patera may have been hydrothermal and provided habitable environments for an extended period, perhaps millions of years or more, supported by locally enhanced geothermal gradients. Sixty percent of all NHA basins exhibit terminal deposits, which may preserve a record of this habitability, and we expect that while the habitability of these lakes varies greatly depending on age and duration of sustained water activity, overall habitability would increase with proximity to the volcanic center.

Acknowledgments

This research was supported by a senior postdoctoral research fellowship awarded to H.I.H. by the NASA Postdoctoral Program (NPP) at Ames Research Center, administered initially by ORAU and USRA through a contract with NASA. V.C.G. is supported by MRO HiRISE Co-I funds and also by SETI Institute's NASA Astrobiology Institute Grant #NNX15BB01A. N.H.G. is supported by her research assistantship to V.C.G. We are grateful for the comments of the anonymous reviewer who helped us improve the article.

Author Disclosure Statement

No competing financial interests exist.

References

Ansan, V., Loizeau, D., Mangold, N., Le Mouélic, S., Carter, J., Poulet, F., Dromart, G., Lucas, A., Bibring, J-P., Gendrin, A., Gondet, B., Langevin, Y., Masson, P.h., Murchie, S.,

Mustard, J.F., and Neukum, G. (2011) Stratigraphy, mineralogy, and origin of layered deposits inside Terby crater, Mars. *Icarus* 211:273–304.

Ariztegui, D., Gilli, A., Anselmetti, F.S., Goñi, R.A., Belardi, J.B., and Espinosa, S. (2010). Lake-level changes in central Patagonia (Argentina): crossing environmental thresholds for Lateglacial and Holocene human occupation. *J Quat Sci* 25: 1092–1099.

Aureli, K.L., Goudge, T.A., Head, J.W., and Fassett, C.I. (2014) Classification of candidate impact crater-hosted closed-basin lakes on Mars. In *45th Lunar and Planetary Science Conference #2369*. Houston, TX.

Baker, V.R., Strom, R.G., Gulick, V.C., Kargel, J.S., and Komatsu, G. (1991) Ancient oceans, ice sheets and the hydrological cycle on Mars. *Nature* 352:589–594.

Bernhardt, H., Hiesinger, H., Ivanov, M., Ruesch, O., Erkeling, G., and Reiss, D. (2016) Photogeologic mapping and the geologic history of the Hellas basin floor, Mars. *Icarus* 264: 407–442.

Bohacs, K.M., Carroll, A.R., Neal, J.E.,, and Mankiewicz, P.J. (2000) Lake-basin type, source potential, and hydrocarbon character: an integrated-sequence-stratigraphic–geochemical framework. In *Lake Basins Through Space and Time*, edited by E.H. GierlowskiKordesch and K. R. Kelts, AAPG Studies in Geology 46, pp. 3–34.

Cabrol, N.A. and Grin, E.A. (1999) Distribution, classification, and ages of Martian impact crater lakes. *Icarus* 142: 160–172.

Cabrol, N.A. and Grin, E.A. (2001) The evolution of lacustrine environments on Mars: is Mars only hydrologically dormant? *Icarus* 149:291–328.

Cabrol, N.A. and Grin, E.A., editors. (2010) *Lakes on Mars*. Elsevier, Amsterdam, p. 390.

Carter, J., Loizeau, D., Mangold, N., Poulet, F., and Bibring, J.-P. (2015) Widespread surface weathering on early Mars: a case for a warmer and wetter climate. *Icarus* 248:373–382.

Chivian D., Brodie, E.L., Alm, E.J., Culley, D.E., Dehal, P.S., DeSantis, T.Z., Gihring, T.M., Lapidus, A., Lin, L.-H., Lowry, S.R., Moser, D.P., Richardson, P., Southam, G., Wanger, G., Pratt, L.M., Andersen, G.L., Hazen, T.C., Brockman, F.J., Arkin, A.P., and Onstott, T.C. (2008) Environmental genomics reveals a single-species ecosystem deep within Earth. *Science* 322. doi:10.1126/science.1155495

Costelloe, J.F., Irvine, E.C., Western, A.W., and Herczeg, A.L. (2009) Groundwater recharge and discharge dynamics in an arid-zone ephemeral lake system, Australia. *Limnol Oceanogr* 54:86–100.

Craddock, R.A. and Maxwell T.A. (1993) Geomorphic evolution of the Martian highlands through ancient fluvial processes. *J Geophys. Res* 98(E2):3453–3468.

Crown, D.A. and Greeley, R. (2007) Geologic Map of MTM-30262 and -30267 Quadrangles, Hadriaca Patera Region of Mars. USGS Scientific Investigations Map 2936, Atlas Of Mars: MTM–30262 and–30267 Quadrangles U.S. Department of the Interior, U.S. Geological Survey.

Crown, D.A., Bleamaster III, L.F., and Mest, S.C. (2005) Styles and timing of volatile-driven activity in the eastern Hellas region of Mars. *J Geophys Res* 110:E12S22.

Daubar, I.J. and Kring, D.A. (2001) Impact-induced hydrothermal systems: heat sources and lifetimes. In 32th Lunar and Planet Science Conference, abstract #1727, Houston.

De Hon, R.A. (1992) Martian lake basins and lacustrine plains. *Earth Moon Planets* 56:95–122.

Dehouck, E., Mangold, N., Le Mouélic, S., Ansan, V., and Polet, F. (2010) Ismenius Cavus, Mars: a deep paleolake with phyllosilicate deposits. *Planet Space Sci* 58:941–946.

de Villiers, G., Kleinhans, M.G., and Postma G. (2013) Experimental delta formation in crater lakes and implications for interpretation of Martian deltas. *J Geophys Res Planets* 118: 651–670.

Di Achille, G. and Ori, G.G. (2008) Complex intermontaine glacial systems in Arabia Terra, Mars: evidence for an Amazonian proglacial lake with associated glacilacustrine deposits. In 39th Lunar and Planet Science Conference, abstract #2096, Houston.

Ericksen, G.E. (1987) *Geology and Resources of Salars in the Central Andes*. USGS Open-File Report 88-210.

Fassett, C.I. and Head, J.W. (2008) Valley network-fed, openbasin lakes on Mars: distribution and implications for Noachian surface and subsurface hydrology. *Icarus* 198: 37–56.

Forester, R.M., Miller, D.M., and Pedone, V.A. (2003) Ground water and ground-water discharge carbonate deposits in warm deserts. *Land of the Lost Lakes,* edited by R.E. Reynolds. California State University, Desert Studies Consortium, Fullerton, California.

Forsythe, R.D. and Blackwelder, J.R. (1998) Closed drainage crater basins of the Martian highlands: constraints on the early Martian hydrologic cycle. *J Geophys Res* 103(E13): 31421–31431.

Goudge, T.A., Head, J.W., Mustard, J.F., and Fassett, C.I. (2012) An analysis of open-basin lake deposits on Mars: evidence for the nature of associated lacustrine deposits and post-lacustrine modification processes. *Icarus* 219:211–229.

Goudge, T.A., Aureli, K.L., Head, J.W., Fassett, C.I., and Mustard, J.F. (2015) Classification and analysis of candidate impact crater-hosted closed-basin lakes on Mars. *Icarus* 260: 346–367.

Grant, J.A., Irwin III, R.P., Wilson, S.A., Buczkowski, D., and Siebach, K. (2011) A lake in Uzboi Vallis and implications for Late Noachian–Early Hesperian climate on Mars. *Icarus* 212:110–122.

Greeley, R. (1994) *Planetary Landscapes*, 2nd ed., Springer-Science+Business Media, New York, London.

Gulick, V.C. (1998) Magmatic intrusions and a hydrothermal origin for fluvial valleys on Mars. *J Geophys Res* 103(E8): 19365–19387.

Gulick, V.C. (2001) Origin of the valley networks on Mars: a hydrological perspective. *Geomorphology* 37:241–268.

Gulick, V.C. and Baker V.R. (1990) Origin and evolution of valleys on Martian volcanoes. *J Geophys Res* 95(B9):14325–14344.

Hamilton, J.C., Lundblad, S., Clark, D.L., Purves, N.G., Milovsoroff, C.T., and Thomas, N. (2015) *Ausonia Cavus and Kasei Valles: Complementary Exploration Zone Sites for Biology, Geology and ISRU*. First Landing Site/Exploration Zone Workshop for Human Missions to the Surface of Mars #1045.

Hargitai, H.I. and Gulick, V. (2017) *Knobby Terrains at the Sources of the Navua-Hadriacus Drainage Systems on Mars: What are the Knobs?* LPSC 48. Houston, March 20–24, #1763.

Hargitai, H., Gulick, V., and Glines, N. (2017) Discontinuous drainage systems formed by precipitation and ground-water outflow in the Navua Valles and Southwest Hadriacus Mons, Mars. *Icarus.* DOI://10.1016/j.icarus.2017.03.005

Hargitai, H., Gulick, V., and Glines, N. (2018) The Geology of the Navua Valles Region of Mars. *J Maps* doi:10.1080/17445647.2018.1496858

Hartmann, W.K. and Neukum, G. (2001) Cratering chronology and the evolution of Mars. *Space Sci Rev* 96:165–194.

Hoke, M.R.T., Hynek, B.M., and Tucker, G.E. (2011) Formation timescales of large Martian valley networks. *Earth Planet Sci Lett* 312:1–12.

Irwin, R.P., III, Maxwell, T.A., Howard, A.D., Craddock, R.A., and Leverington, D.W. (2002) A large Paleolake Basin at the Head of Ma'adim Vallis, Mars. *Science* 296. doi:10.1126/science.1071143

Irwin, R.P., III, Howard, A.D., Craddock, R.A., and Moore J.M. (2005) An intense terminal epoch of widespread fluvial activity on early Mars: 2. Increased runoff and paleolake development. *J Geophys Res* 110:E12S15.

Ivanov, B.A. (2001) Mars/Moon cratering rate ratio estimates. *Chronol Evol Mars* 96:87–104.

Jankowski, D.G. and Squyres, S.W. (1993) ''Softened'' impact craters on Mars: implications for ground ice and the structure of the Martian Megaregolith. *Icarus* 106:365–379.

Kerber, L., Dickson, J.L., Head, J.W., and Grosfils, E.B. (2016) Polygonal ridge networks on Mars: diversity of morphologies and the special case of the Eastern Medusae Fossae Formation. *Icarus* 281:200–219.

Kereszturi, A. and De Hon, R. (2014) Lacustrine features (Mars). In *Encyclopedia of Planetary Landforms*, edited by H. Hargitai and A. Kereszturi. Springer Science+Business Media, New York. doi:10.1007/978-1-4614-9213-9_212-1

Kneissl, T., van Gasselt, S., and Neukum, G. (2011) Map-projection-independent crater size-frequency determination in GIS environments—new software tool for ArcGIS. *Planet Space Sci* 59:1243–1254.

Kreslavsky, M.A. and Head, J.W. (2002) Fate of outflow channel effluents in the northern lowlands of Mars: the Vastitas Borealis formation as a sublimation residue from frozen ponded bodies of water. *J Geophys Res* 107(E12):5121.

Leverington, D.W. and Maxwell, T.A. (2004) An igneous origin for features of a candidate crater-lake system in western Memnonia, Mars. *J Geophys Res* 109:E06006.

Malin, M.C. and Edgett, K.S. (2000) Sedimentary rocks of early Mars. *Science* 290:1927–1937.

Mest, S.C. and Crown, D.A. (2001) Geology of the Reull Vallis Region, Mars. *Icarus* 153:89–110.

Michael, G.G. and Neukum, G. (2010) Planetary surface dating from crater size–frequency distribution measurements: partial resurfacing events and statistical age uncertainty. *Earth Planet Sci Lett* 294:223–229.

Michael, G.G., Platz, T., Kneissl, T., and Schmedemann, N. (2012) Planetary surface dating from crater size–frequency distribution measurements: spatial randomness and clustering. *Icarus* 218:169–177.

Moore, J.M. and Wilhelms, D.E. (2001) Hellas as a Possible Site of Ancient Ice-Covered Lakes on Mars. *Icarus* 154:258–276.

Musiol, S., Cailleau, B., Platz, T., Kneissl, T., Dumke, A., and Neukum, G. (2011) Outflow activity near Hadriaca Patera, Mars: fluid-tectonic interaction investigated with High Resolution Stereo Camera stereo data and finite element modeling. *J Geophys Res* 116:E08001.

Mustard, J.F., Ehlmann, B.L., Murchie, S.L., Poulet, F., Mangold, N., Head, J.W., Bibring, J.-P., and Roach, L.H. (2009) Composition, morphology, and stratigraphy of Noachian Crust around the Isidis basin. *J Geophys Res* 114:E00D12.

Neukum, G., Ivanov, B.A., and Hartmann, W.K. (2001) Cratering records in the inner solar system in relation to the lunar reference system. Space Science Reviews 96:55. https://doi.org/10.1023/A:1011989004263

Nichols, G. (2009) *Sedimentology and Stratigraphy*. Wiley-Blackwell, Oxford.

Ori, G.G., Marinangeli, L., and Baliva, A. (2000) Terraces and Gilbert-type deltas in crater lakes in Ismenius Lacus and Memnonia (Mars). *J Geophys Res* 105(E7):17629–17641.

Osinski, G.R., Tornabene, L.L., Banerjee, N.R., Cockell, C.S., Flemming, R., Izawa, M.R.M., McCutcheon, J., Parnell, J., Preston, L.J., Pickersgill, A.E., Pontefract, A., Sapers, H.M., and Southam, G. (2013) Impact-generated hydrothermal systems on Earth and Mars. *Icarus* 224:347–363.

Parker, T.J., Saunders, R.S., and Schneeberger, D.M. (1989) Transitional morphology in the west Deuteronilus Mensae region of Mars: implications for modification of the lowland/upland boundary. *Icarus* 82:111–145.

Robbins, S.J. and Hynek, B.M. (2012) A new global database of mars impact craters ≥1 km: 1. Database creation, properties, and parameters. *J Geophys Res Planets* 117:E05004.

Robbins, S.J., Di Achille, G., and Hynek, B.M. (2011) The volcanic history of Mars: high-resolution crater-based studies of the calderas of 20 volcanoes. *Icarus* 211:1179–1203.

Rodriguez, J.A.P., Zarroca, M., Linares, R., Gulick, V.C., Weitz, C.M., Yan, J., Fairén, A.G., Miyamoto, H., Platz, T., Baker, V., Kargel, J., Glines, N., and Higuchi, K. (2016) Groundwater flow induced collapse and flooding in Noctis Labyrinthus, Mars. *Planet Space Sci* 124:1–14.

Salese, F., Ansan V., Mangold N., Carter J., Ody A., Poulet F., and Ori, G.G. (2016) A sedimentary origin for intercrater plains north of the Hellas basin: implications for climate conditions and erosion rates on early Mars. *J Geophys Res Planets* 121. doi:10.1002/2016JE005039

Sanford, W.E. and Wood, W.W. (1991) Brine evolution and mineral deposition in hydrologically open evaporite basins. *Am J Sci* 291:687–710.

Schon, S.C., Head, J.W., and Fassett, C.I. (2012) An overfilled lacustrine system and progradational delta in Jezero crater, Mars: implications for Noachian climate. *Planet Space Sci* 67:28–45.

Scott, D.H., Chapman, M.G., Rice, J.W. Jr, and Dohm, J.M. (1992) New evidence of lacustrine basins on Mars—Amazonis and Utopia Planitiae. *Lunar Planet Sci* 22:53–62.

Scott, D.H., Dohm, J.M., and Rice, J.M. (1995) *Map of Mars Showing Channels and Possible Paleolakes Basins (1: 30,000,000)*. US Geol Surv Misc Inves Map I-2461.

Smith, D.E., Zuber, M.T., Neumann, G.A., Guinness, E.A., and Slavney, S. (2003) Mars Global Surveyor Laser Altimeter Mission Experiment Gridded Data Record, NASA Planetary Data System, MGS-M-MOLA-5-MEGDR-L3-V1.0.

Soare, R.J., Osinski, G.R., and Roehm, C.L. (2008) Thermokarst lakes and ponds on Mars in the very recent (late Amazonian) past. *Earth Planet Sci Lett* 272:382–393.

Tyler, S.W., Muñoz, J.F., and Wood, W.W. (2006) The response of Playa and Sabkha hydraulics and mineralogy to climate forcing. *Ground Water* 44:329–338.

Warren, J.K. (2016) *Evaporites. A Geological Compendium*. Springer, p. 265. doi:10.1007/978-3-319-13512-0

WDNR. (2001) *The State of the Upper Fox River Basin*. October, 2001 WT-665-2001. A Report by the Wisconsin Department of Natural Resources in Cooperation with the Upper Fox River Basin Partnership Team and Stakeholders. Available

online at www.greenlakeassociation.com/glaw/wp-content/uploads/2010/12/upfox1.pdf

Weiss D.K. and Head, J.W. (2015) Crater degradation in the Noachian highlands of Mars: assessing the hypothesis of regional snow and ice deposits on a cold and icy early Mars. *Planet Space Sci* 117, 401–420.

Werner, S.C. (2009) The global martian volcanic evolutionary history. *Icarus* 201:44–68.

Williams, D.A., Greeley, R., Zuschneid, W., Werner, S.C., Neukum, G., Crown, D.A., Gregg, T.K.P., Gwinner, K., and Raitala, J. (2007) Hadriaca Patera: insights into its volcanic history from Mars Express High Resolution Stereo Camera. *J Geophys Res* 112:E10004.

Wilson, S.A., Howard, A.D., Moore, J.M., and Grant, J.A. (2007) Geomorphic and stratigraphic analysis of Crater Terby and layered deposits north of Hellas basin, Mars. *J Geophys Res* 112:E08009.

Wilson, S.A., Moore, J.M., Howard, A.D., and Wilhelms. D.E. (2010) Evidence for ancient lakes in the Hellas region. In *Lakes on Mars*, edited by N.A. Cabrol and E.A. Grin. Elsevier BV, pp 195–222. doi:10.1016/B978-0-444-52854-4.00007-6

Wilson, S.A., Howard, A.D., Moore, J.M., and Grant, J.A. (2016) A cold-wet middle-latitude environment on Mars during the Hesperian-Amazonian transition: evidence from northern Arabia valleys and paleolakes. *J Geophys Res Planets* 121:1667–1694.

Wray, J.J., Milliken, R.E., Dundas, C.M., Swayze, G.A., Andrews-Hanna, J.C., Baldridge, A.M., Chojnacki, M., Bishop, J.L., Ehlmann, B.L., Murchie, Scott L., Clark, R.N., Seelos, F.P., Tornabene, L.L., and Squyres, S.W. (2011) Columbus crater and other possible groundwater-fed paleolakes of Terra Sirenum, Mars. *J Geophys Res* 116:E01001.

Address correspondence to:
Henrik I. Hargitai
ELTE Eötvös Loránd University
Budapest, Hungary

E-mail: hargiatih@caesar.elte.hu

Submitted 4 January 2018
Accepted 15 March 2018

Abbreviations Used

LDM = latitude-dependent mantle
LTD = light-toned deposit
NHA = Navua Valles–Hadriacus Mons–Ausonia Montes